UNIVERSITY OF TARTU
Faculty of Science and Technology
Institute of Technology

Turan Badalli

Inducible protein degradation in *Saccharomyces cerevisiae*

Bachelor's Thesis (12 ECTS)

Curriculum Science and Technology

Supervisors:
Rait Kivi PhD
Kaidi Möll MSc.

Tartu 2020

Inducible Protein Degradation in *Saccharomyces cerevisiae*

Abstract:

Recently, several synthetic biology toolboxes have been developed to be used in *S.cerevisiae*. The application of such toolbox components helps to improve bioproduction of desired chemicals or heterologous enzymes. In this work, we designed a Clb3-CDC28 (cyclin-cyclin dependent kinase) specific degron module that can be used as a synthetic biology tool in order to direct the metabolic dynamics of *S.cerevisiae*. The results showed that the degradation of such degron module conjugated proteins are mediated by the phosphorylation of the CDC28 target residues at Cln2 degron domain and this phosphorylation is predominantly carried out by Clb3-CDC28 complex which makes the degradation controllable. However, we also showed that expression of Clb3-CDC28 is not the only factor that drives the degradation of degron module conjugated proteins by leaving an empty room to improve the controllability of the system.

Keywords: Synthetic Biology, Degron module, Phosphorylation, Degradation, Cyclin, Cyclin dependent kinase

CERCS: P310 Proteins, Enzymology

Indutseeritav valkude lagundamine pagaripärmis

Pagaripärmi jaoks on viimasel ajal arendatud mitmeid sünteetilise bioloogia tööriistakaste. Taoliste tööriistakastide abil saab rakkudes toota mitmeid vajalikke kemikaale ja ensüüme. Bakalaureuse töö käigus disainiti Clb3-CDC28 spetsiifiline degronimoodul, mille abil saab mõjutada rakkude metabolismi *S. cerevisea*'s. Töö tulemusel selgus, et Clb3-CDC28 spetsiifilise fosforüülimisega saab mõjutada Cln2 degronil põhineva mooduliga seotud valkude tasemeid. Samas selgus, et degronimooduli lisamine valkudele mõjutab nende taset sõltumata Clb3-CDC28 indutseerimisest, mistõttu tuleb tulevikus antud süsteemi täiustada.

Märksõnad: Sünteetiline bioloogia, Degronimoodul, Fosforüülimine, Valkude lagundamine, Tsükliin, Tsükliinsõltuv kinaas

CERCS: P310 Proteiinid, Ensüümid

TABLE OF CONTENTS

TERMS, ABBREVIATIONS AND NOTATIONS

APC/C - Anaphase-Promoting Complex or Cyclosome

CDC28 – Cyclin-dependent kinase 1

CDK- Cyclin-dependent kinase

EDTA - Ethylenediaminetetraacetic acid

HRP – Horse radish peroxidase

OD – Optical density

PNF – Short linear Clb3-CDC28 dependent docking motif

RXL - Short linear Clb5-dependent docking motif from with consensus sequence of K/R-x-L- φ or K/R-x-L-xφ sequence

SCF - Skp, Cullin, F-box containing complex

TAE buffer - Tris-acetate-EDTA buffer

TE buffer - Tris-EDTA buffer

VLLPP – Short linear Cln2-dependent docking motif from Sic1 with VLLPP amino acid

YPD – Yeast extract peptone dextrose

INTRODUCTION

The cell cycle is a complex series of events, starting with cell growth which is followed by DNA duplication and ending up giving rise to two new daughter cells as a result of the cytoplasmic division, cytokinesis. To complete the cell cycle, a cell is supposed to pass through four different phases: G1, S, G2, and M. The cell cycle control system mediates the cell cycle progression to be in a highly regulated fashion by controlling the transition through the successive cell cycle phases by the functioning of its main component, cyclin-dependent kinase (CDK). CDKs regulate cell cycle progression by inducing downstream processes, either promoting their activation or inactivation. In budding yeast, cyclin-dependent kinase CDC28 is the main regulator of the cell cycle.

As the name implies, in order to be activated CDK requires binding of a regulatory subunit, cyclin. In addition to activating CDK, cyclin defines the substrate specificity of cyclin-CDK complexes by recognizing specific docking motif of the substrate. For example, phosphorylation of the target proteins with the PxF docking motif are only recognized by Clb3-CDC28 complex. In *S. cerevisiae* there are 9 cyclins that participate in the cell cycle regulation by forming distinct cyclin-CDC28 complexes and they can be divided into four different groups (G1, G1/S, S, M). Highly regulated expression and degradation of cyclins by ubiquitin-proteasome system (UPS) results in the oscillatory cyclin levels which mediate fluctuation in CDK activity to run the cell cycle. Fundamentally, UPS comprises sequentially working three enzymes: ubiquitin-activating enzyme E1, ubiquitin-conjugating enzyme E2, ubiquitin-protein ligase E3. There are two related multisubunit E3 enzyme complexes that perform degradation of cell cycle regulatory components: SCF (Skp1/cullin/F-box protein) and APC/C (anaphase-promoting complex or cyclosome). The SCF complex controls G1/S and G2/M transitions, while APC/C mediates metaphase-anaphase transition by tagging specific proteins with ubiquitin for degradation. There are two types of SCF that are involved in cell cycle regulation: SCF^{Grr1} and SCF^{Cdc4}. SCF^{Cdc4} is nuclear enzyme, while SCF^{Grr1} is found in both cytoplasm and nucleus. In order to be recognized by SCF enzyme complexes, target proteins must be phosphorylated at their phosphodegron site, which is a protein domain that contains CDC28 phosphorylation sites.

In this work, we are trying to create a controllable protein degradation system by designing Clb3-CDC28 specific degron module that can be used as a synthetic biology tool. In order to check

implementability of the system, we analyze degradation efficiency of such module tagged metabolic proteins in model organism *S.cerevisiae's* cytoplasm.

1. LITERATURE REVIEW

1.1. Cell Cycle

The ability to grow and reproduce is a principal property of living things, despite this fact, the growth of single cells is essentially restricted. The accumulation of synthesized biomolecules is the driving force to increase the cell volume by pushing the plasma membrane to expand to prevent the bursting of the cell. But as it's mentioned above, the cells are deprived of unlimited growth ability; the rise of the cell volume leads to an accompanying drop in the surface area/volume ratio which restricts effective exchange with the environment. Henceforth, cell growth is generally accompanied by cell division, whereby one cell gives rise to two new daughter cells (Hardin, J., 2017).

The theory of cell division has been initially settled in the nineteenth century and it conveys a significant message for the progression of life. Every single living creature, from the unicellular bacterium to the multicellular warm-blooded animal, is a result of rehashed rounds of cell growth and division reaching out back to the beginnings of life on Earth more than three billion years prior (Alberts, 2015).

The eukaryotic cell cycle is generally divided into four consecutive phases: G1, G2, and S. The pre mitotic phases, G1, S, and G2 together are called interphase. There are 2 major phases of the cell cycle, the first phase is defined by the duplication of the vast amount of DNA in the chromosomes which is called S phase (S for DNA synthesis), and the second phase is defined by the segregation of the chromosome copies into two genetically identical cells which is called M phase (M for mitosis). M phase involves 2 significant events: nuclear division, or mitosis, during which the duplicated chromosomes are spread equally into a pair of daughter nuclei; and cytoplasmic division, or cytokinesis when the cell cytoplasm is divided into two daughter cells (Alberts, 2015).

Most eukaryotic cells require considerably more time to grow and duplicate their mass of biomolecules and organelles than they require to copy their chromosomes and divide. Halfway to

permit time for growth, most cell cycles have 2 gap phases: G1 phase (gap 1) between M and S phases; G2 (gap 2) phase between S phase and mitosis (Alberts, 2015).

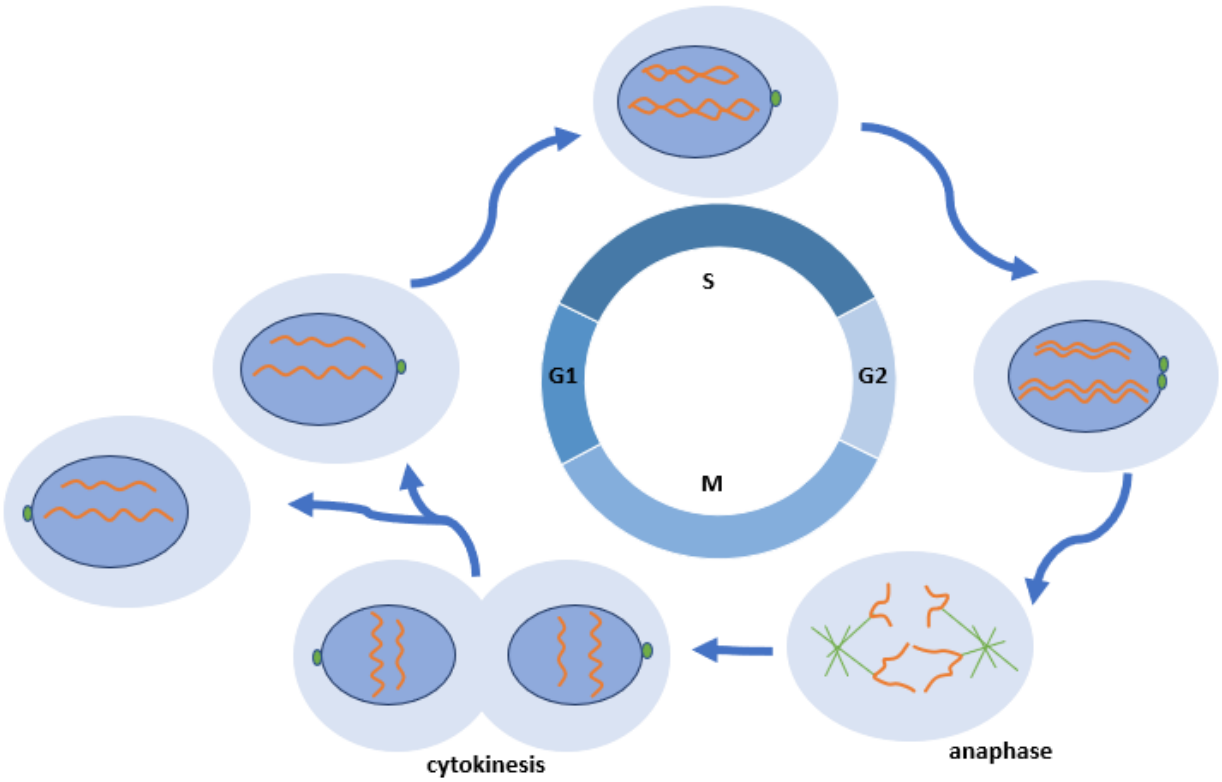

Figure 1. Cell Cycle.

The main events of the cell cycle are DNA duplication that takes place in S phase, followed by the segregation of replicated chromosomes in anaphase and cytoplasmic division which is called cytokinesis. The last two events are collectively called M phase. G1 is a gap phase between M and S phases, while G2 is the gap phase between S and M phases (The figure has been modified from Morgan, 2007).

The two gap phases provide the cell with a sufficient amount of time to keep track of internal and external environments to guarantee that conditions are appropriate and preparations are complete before the cell commits itself to cell division and the accompanying significant changes of S phase and mitosis. The length of the G1 phase can shift enormously relying upon extracellular

signals from the environment and other cells. In case of adverse extracellular conditions, cells defer progress through G1 and may even enter a particular resting state known as G0 (gap 0), in which they can stay for starting from several days to few years before proceeding with the next stages of the cell cycle. In fact, most of the cells in multicellular organisms remain in G0 until they or the organism dies. In case of favorable extracellular conditions and signals from the other cells for the direction to grow and divide are available, cells in early G1 or G0 progress through a checkpoint near the end of G1 known as Start for yeasts. After passing the Start point, the cells are supposed to continue with DNA replication, regardless of whether extracellular signals that invigorate cell growth and division are put off (Alberts, 2015).

1.2. Cell Cycle Control System

Strictly controlled timing and rotation of DNA replication and chromosome segregation are critical for the steadfast distribution of the eukaryotic genome and the rising of two new viable cells (Swaffer et al., 2016). The cell-cycle control system is a rigidly programmed regulatory network that consists of series of biochemical switches that trigger the progression through the three essential checkpoints (Start, which defines the entry into the cycle in late G1; G2/M, which is the control point for entry into the mitosis; metaphase-anaphase transition, which is the checkpoint for the progression with the final events of mitosis) of the cell cycle by providing a fixed amount of time for the completion of each cell-cycle event (Morgan, 2007; Alberts, 2015).

The cell-cycle events are controlled by members of the protein kinase family known as cyclin-dependent kinases (CDKs) (Alto, 1995). CDKs are small protein kinases (34-40 kDa) which are involved in several cellular functions such as cell cycle regulation, transcription, epigenetic regulation, stem cells self-renewal (Morgan, 2007; Malumbres et al., 2009; Lim & Kaldis, 2013). The main reason behind such versatility of CDKs is the functionality, to catalyze the phosphorylation of hundreds of target proteins that trigger a sequence of coordinated molecular events (Kõivomägi et al., 2014). Protein phosphorylation is the most frequent, reversible post-translational protein modification in which amino acid residue is phosphorylated by a protein kinase by the addition of covalently bound phosphoryl group in order to activate, deactivate or modify the function of the target protein (Cohen, 2002; Vlastaridis et al., 2017).

However, in order to be activated, CDK is supposed to associate with another component of the cell cycle control system, cyclin (Rev et al., 1997). Fundamentally, cyclins are stage-specific regulatory subunits of CDK, which means that each kind of cyclin is expressed in the different stages of the cell cycle, by leading to the formation of stage-specific CDK-cyclin complexes (Örd & Loog, 2019; Rev et al., 1997). The formation of these multistage-specific complexes ensures a regulated progression of the cell cycle (Morgan, 2007).

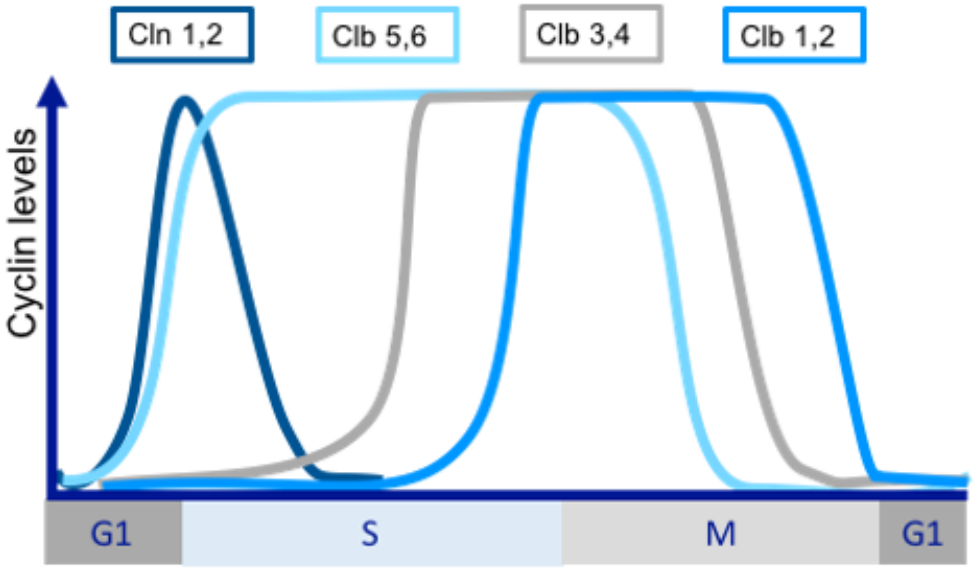

Figure 2. Cyclin level during the cell cycle.
The graph above shows the abundance of different cyclins during different phases of the cell cycle. Oscillations in cyclin levels give rise to the fluctuations in Cdk1 activity. Concentrations of cyclins are mainly controlled by their expression and degradation (The figure has been modified from Morgan, 2007).

Overall, the cell-cycle control system is special with its own distinctive properties: having a binary (on/off) switches while initiating events in a complete and irreversible style; being notably

robust and trustworthy due to being able to run effectively under different conditions even if some components fail; being extremely adaptable and modifiable to fit specific cell types (Alberts, 2015).

1.3. CDC28 structure, activity, regulation, and cyclins

The model organism, *S.cerevisiae* contains six different CDKs in itself which can be divided into two groups: first, CDKs that make a complex with several cyclins to regulate cell cycle; second, CDKs whose catalytic activity is stimulated by single cyclin leading its involvement in the regulation of transcription. CDC28 and Pho85 are the members of the first group of CDKs family in the model organism Saccharomyces cerevisiae (Malumbres et al., 2009). Among first group CDKs, CDC28 is a main regulator of the budding yeast cell cycle, while keeping its reputation as being the best-studied cyclin-dependent protein kinase so far (Mendenhall & Hodge, 1998).

CDC28 is a proline-directed serine/threonine-protein kinase that can recognize the substrates with both optimal consensus phosphorylation motifs (S/T-P-x-K/R) and suboptimal consensus sites (S/T-P) while phosphorylating the latter one much less efficiently (Kõivomägi et al., 2014; Mendenhall & Hodge, 1998; Songyang et al., 1994). Here, S/T stands for serine or threonine which is supposed to be phosphorylated by CDC28, while P represents proline, and K/R stands for basic amino acid lysine (K) or arginine (R) (Morgan, 2007).

As all other protein kinases, CDC 28 is comprised of a smaller N-terminal lobe, dominated by beta sheets and the large PSTAIRE helix, and a larger C-terminal lobe which is structurally built up primarily of α-helixes (Mendenhall & Hodge, 1998; Morgan, 2007; Rev et al., 1997). The hydrophobic nitrogenous base of ATP binds tightly into the hydrophobic patch within the cleft between the lobes by leading the phosphoryl orientation to be outward, toward the mouth of the cleft (Rev et al., 1997). In the active conformation of CDC28, the protein substrate binds presumably at the entrance of the cleft, interacting principally with the C-terminal lobe surface, to permit contact with the γ – phosphate of ATP. Nearby side chains catalyze the transfer of γ – phosphate on the hydroxyl oxygen of the protein substrate serine or threonine sidechains. Two

types of modification on the catalytic subunit of CDC28 makes them inactive in the absence of cyclin, by hindering its ability to catalyze the phosphotransfer reaction. Firstly, flexible activation loop or T-loop rises from C-terminal and prevents the binding of protein substrate on the active site cleft. Secondly, in the inactive state of CDC28, the amino acids involved in ATP phosphate transfer are incorrectly positioned. Partially, it's due to the misorientation of small L12 helix which goes under the structural change upon cyclin binding by leading the PSTAIRE helix of the upper lobe to move inward which in turn orientates the residues that interact with the phosphate of ATP (Morgan, 2007; Rev et al., 1997).

As the name implies, CDC28 requires cyclin binding to be activated (Galderisi et al., 2003). According to the expression timing and the role in cell cycle progression, the cyclins of *S.cerevisiae* are divided into four classes: G1 phase (Cln3), G1/S phase (Cln1 and Cln2), S phase (Clb5 and Clb6), M phase (Clb1, Clb2, Clb3, and Clb4) (Edgington & Futcher, 2001; Morgan, 2007).

Unlike other cyclins, the only G1 cyclin, Cln3 is not periodically expressed during the cell cycle while there is a small rise in M/G1 border (Blake & Cross, 1993; Tyers et al., 1993). Cln3-CDC28 allows the cells to pass through Start, in the other words, G1/S transition, via inducing the transcription of SBF and MBF transcription factors (Dirick et al., 1992; Nasmyth and Dirick, 1991). Such transcription factors induce the expression of at least 200 cell-cycle regulated genes in the late G1, including, Cln1, Cln2, Clb5, and Clb6 (Spellman et al., 1998). For the understanding of the Cln3 function, some further studies have been done on differentially mutated Cln3 strains. The strains with increased Cln3 stability show a small cell size, while cln3*Δ* strains have an enlarged cell size and extended G1 period but have a normal growth rate due to the compensation by other cell cycle components (F. R. Cross, 1988; Dirick et al., 1995; Stueland et al., 1993). Due to less abundancy and lower specific activity of CDC28 in comparison to Cln1 and Cln2, Cln3 is thought to have a unique role in G1 as an activator of Cln1 and Cln2 (Levine et al., 1996; Tyers et al., 1993).

Unlike Cln3, the expression of G1/S cyclins, Cln1, and Cln2, oscillate during the cell cycle. Expression peaks at the late G1 phase and it is enhanced by their own expression via a positive

feedback loop and protein levels start to decrease at the beginning of the S phase (F. F. Cross, 1991; Morgan, 2007; *Positive Feedback in the Activation of G1 Cyclins in Yeast.Pdf*, n.d.; Skotheim et al., 2009). There are several functions in the cell cycle that Cln1 and Cln2 are responsible for, such as stimulation of DNA synthesis, promotion of budding and spindle body duplication, repression of the anaphase-promoting complex (APC), and phosphorylation of CDC28 inhibitors Far1 (Cln-CDC28 inhibitor) and Sic1 (Clb-CDC28 inhibitor) leading to their destruction via ubiquitin-mediated proteolysis(Lew and Reed, 1995; Haase et al., 1991; Cross, 1995; Henchoz et al., 1997; Peter et al., 1993; Schneider et al., 1996; Schwob et al., 1994; Tyers et al., 1991; Tyers et al., 1993; Edgington & Futcher, 2001; Mendenhall & Hodge, 1998).

Despite all these functions, the *cln1 cln2* double deletion mutant is viable. The main reason behind viability in such a case is the other cyclins, Clb5, Clb6 (CDC28 substrate), and Pcl1 and Pcl2 (Pho85 substrate), which can substitute the functions of Cln1 and Cln2. This statement can be proved by the fact that *cln1 cln2 clb5 clb6* and *cln1 cln2 pcl1 pcl2* mutants are inviable and arrest with unbudded cells and unreplicated DNA (Edgington & Futcher, 2001; Schwob and Nasmyth, 1993). Similarly, *cln1 cln2 cln3* triple mutant also showed inviability, which is described by the deprived expression of Clb5, Clb6, Pcl1, and Pcl2, whose transcription should be promoted by Cln3 (Edgington & Futcher, 2001).

At the beginning of the S phase, an increased concentration of Cln1 and Cln2 promotes their own phosphorylation, leading to the subsequent degradation of G1/S cyclins via SCF-ubiquitin ligase complex pathway (Lanker et al., 1996; Tyers et al., 1992).

Nevertheless, being considered as S phase cyclins, CLB5 and CLB6 are coexpressed in the G1 phase with Cln1 and Cln2, keeping their level high until they start to be degraded by anaphase-promoting complex (APC) in M phase? (Epstein & Cross, 1992; Kuhne & Linder, 1993; Schwob, 1993; Morgan, 2007). Consistently, overexpression of CLB5 and CLB6 covers up the *cln1Δ cln2Δ cln3Δ* lethality, while no other B cyclin is able to do so (Basco et al., 1995; Epstein & Cross, 1992; Lew et al., 1991; Schwob, 1993). Under standard circumstances, CLB5 and CLB6 don't perform as G1/S checkpoint controllers due to their inhibition by Sic1 whose degradation is carried out only after Cln1-CDC28 and Cln2-CDC28 cyclin-kinase complexes activity increases and Sic1 is

degraded after phosphorylation by these cyclin-Cdk1 complexes (Barberis, 2012; Schwob et al., 1994).

The main functions of CLB5 and CLB6 are direct stimulation of DNA synthesis, time regulated S phase initiation, repression of Cln-CDC28 activity and degradation of Cdk1 inhibitor Sic1 by its phosphorylation (Basco et al., 1995; Morgan, 2007; Schwob et al., 1994). CLB5 mutants have a longer? S phase and *clb5Δ clb6Δ* double mutant has an extended S-phase initiation delay, however once initiated, S phase progression occurs at normal speed (Epstein & Cross, 1992; Kuhne & Linder, 1993; Schwob, 1993). However, CLB6 mutants show reduced G1 length and small cells size, denoting an early G1/S transition (Basco et al., 1995). In late G1, as Cln-CDC28 complexes starts phosphorylation of Sic1, by leading to activation of Clb-CDC28 complexes, activated Clb-CDC28 complex carries out further phosphorylation of Sic1 inhibitor, causing its recognition and degradation by SCF-Cdc4 ubiquitin-ligase complex (F. R. Cross, 2003; Morgan & Roberts, 2002).

Sequentially, M cyclins are expressed last, CLB3 and CLB4 transcripts appear in the early S phase, while CLB1 and CLB2 are expressed later, at the beginning of G2 phase, by keeping their level high until late anaphase (Epstein & Cross, 1992; Fitch et al., 1992; Ghiara et al., 1991; Jolla, 2021; Kuhne & Linder, 1993). According to the measurements of absolute levels of protein kinase activity in asynchronous cells and mitotically arrested cells, Clb3-CDC28 comprises the majority of CDC28 activity in asynchronous log-phase cultures and Clb2-CDC28 is the major component of mitotically arrested cells (Grandin & Reed, 1993; Schwob, 1993).

Despite such abundancy, *clb3Δ, clb4Δ, and clb3 Δ clb4Δ* do not show any phenotypical change, while *clb3Δ clb4Δ clb5Δ and clb3Δ clb4Δ clb5Δ clb6Δ* mutants are inviable by not being able to make spindles and initiating S phase, respectively (Fitch et al., 1992; Jolla, 2021; Schwob, 1993). However, the larger cell size of *clb2* deletion mutant and the lethality of *clb2Δ clb1Δ* and *clb2Δ clb3Δ* double-mutants indicate phenotypical importance of CLB2 in *S.cerevisiae* (Amon et al., 1993; Epstein & Cross, 1992; Jolla, 2021; Surana et al., 1991).

1.4. Substrate targeting

The main driving force of the cell cycle progression is the promotion of distinct cell cycle events which are controlled by their specific cyclin-CDK complexes (Morgan, 2007). It is mainly due to the specificity of cyclin-CDK complexes which is provided by cyclin in several ways: time-dependent expression, differential sensitivity to cell-cycle regulators, taking CDK to subcellular locations where substrates found, and direct interaction with substrates (Bloom & Cross, 2007; Ubersax & Jr, 2007; Morgan, 2007). In terms of direct cyclin-substrate binding, a short sequence of the substrate called the docking motif facilitates the recognition of substrate by its distinct cyclin-CDK complex (Skotheim, 2019). For example, a substrate with the PxF motif is predominantly recognized by M phase cyclin Clb3, which leads to its phosphorylation by the Clb3-Cdk1 complex, while allowing us to conclude that PxF is Clb3 specific motif (Örd et al., 2020). In addition to PxF, there are 2 other docking motifs, RxL, and VLLPP, that have been discovered so far with their significant roles in cell cycle regulation (F. R. Cross et al., 1999; Kõivomägi et al., 2011; Loog & Morgan, 2005).

S phase cyclins, mainly Clb5 recognizes the substrates as a result of interaction between the hydrophobic patch of the cyclin and RxL motif of the substrate (Morgan, 2007). Research related to the retinoblastoma protein phosphorylation and Orc6 phosphorylation has revealed that the mutations introduced to the RxL docking site or replacing Clb5 with M phase cyclin Clb2, hinders the substrate phosphorylation rate (Adams et al., 1999; Loog & Morgan, 2005; Wilmes et al., 2004). The studies on the Sic1 destruction have shown that mutation of the RxL motif causes a delay in Sic1 degradation (Valk et al., 2012).

On the other hand, the LP motif (enriched in Leu and Pro) is G1/S cyclin specific meaning that substrate with such target sequence is preferentially phosphorylated by Cln1/2-CDC28 complex (Bhaduri & Pryciak, 2011; Kõivomägi et al., 2011). The mechanism is similar to the Clb5-RxL motif interaction, while, recognition site of Cln1/2 is close but separated from hydrophobic patch region (Bhaduri & Pryciak, 2011; Chulman & Indstrom, 1998; Kõivomägi et al., 2011; Loog & Morgan, 2005; Wilmes et al., 2004). Similarly to that of the RxL motif, it has been shown that mutation in the LP motif also brings on delay in Sic1 degradation, by pointing

out the significance of the LP motif for the recognition by Cln1/2-CDC28 complex (Valk et al., 2012).

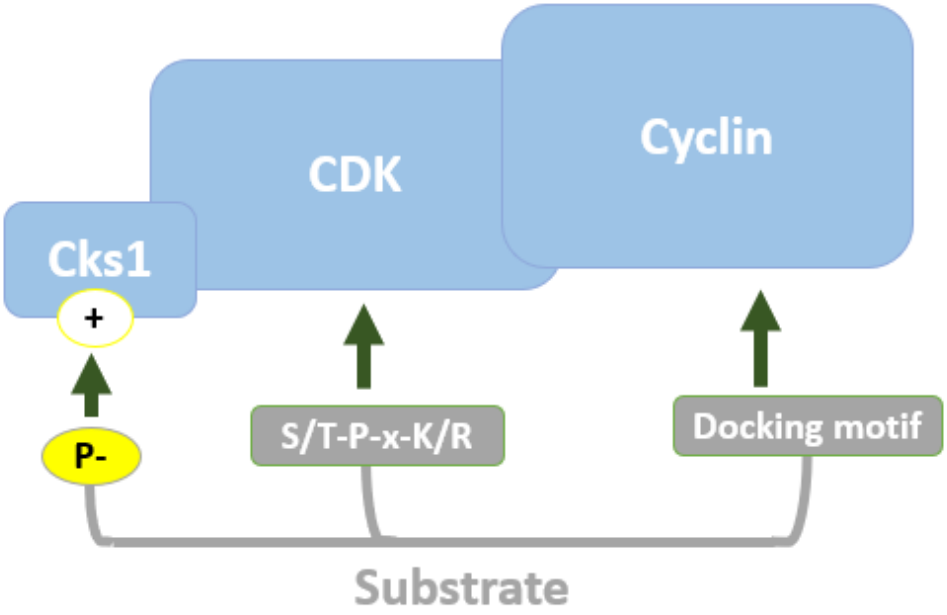

Figure 3. CDK-Cyclin-Cks1 complex. CDK is a proline-directed kinase that phosphorylates a serine/threonine residue in the target protein. S/TP motif with a downstream basic residue (K or R) form an optimal CDK site. Cks1 binds pre-phosphorylated phospho-threonines in the substrate proteins, enhancing CDK activity towards the target protein. Linear cyclin docking motif can specify the targeting, increasing the affinity of specific cyclin-CDK complexes towards the substrate (The figure has been modified from Morgan, 2007).

In addition to cyclin binding, phosphorylation on Thr160, threonine residue adjacent to the kinase active site, is required for CDC28 activity to reach its peak and this regulation is performed by Cks1, which is a regulatory subunit of CDC28 in *S.cerevisiae* (Magill et al., 2010; Morgan, 2007; Rev et al., 1997). In budding yeast, Cks1 binding to the CDC28 occurs prior to the cyclin binding, at the site that is distinct from ATP and cyclin binding sites (Magill et al., 2010; Rédei, 2008). Regarding the phosphorylation order of Cks1-binding consensus sites in the multisite phosphorylation of CDC28 substrates, if such phosphorylation occurs early in the reaction, then

Cks1 causes the phosphorylation of remaining sites in the direction of N to C terminal, with the optimal distance between priming site and secondary phosphorylation site being 12-16 amino acids, as in Sic1 phosphorylation (Magill et al., 2010; Tang & Reed, 1993; Kõivomägi et al., 2013). Comprehensively, T2, T5, and T33 residues of Sic1 enhance its degradation by being used as a priming site for Cks1 regulatory subunit of Clb5-CDC28 (Loog, 2011).

1.5. Protein degradation

1.5.1. Ubiquitin-proteasome system (UPS)

The progression through cell cycle phases should be irreversible which is ensured by the proteolytic degradation of the regulatory subunits of CDK, and the ubiquitin-proteasome system (UPS) is responsible to perform such function (Morgan, 2007; Reed, 2003). Fundamentally, UPS comprises sequentially working three enzymes: ubiquitin-activating enzyme E1, ubiquitin-conjugating enzyme E2, ubiquitin-protein ligase E3 (Manuscript, 2015; Morgan, 2007; Xie et al., 2019).

In the initial step, ordered binding of MgATP and ubiquitin occurs leading to the formation of ubiquitin adenylate intermediate which serves as a donor for ubiquitin-binding through its carboxyl terminus to the sulfhydryl group of cysteine in the active site of E1 (Haas et al., 1982; Mcgrath et al., 1991; Morgan, 2007; Pickart, 2001; Zacksenhaus & Sheinin, 1990). Subsequently, the E1-ubiquitin complex interacts with ubiquitin-conjugating enzyme E2, promoting ubiquitin transfer to the E2 (Morgan, 2007; Pickart, 2001). In the final step, E3 acts in concert with E2-ubiquitin complex to recognize substrate and immediately upon to the recognition, E3 catalyzes the formation of isopeptide bond between C-terminal of ubiquitin and lysine residue of the targeted protein, facilitating ubiquitin transfer (Hurley et al., 2006; Morgan, 2007; Pickart, 2001). Principally, a defined array of ubiquitin is conjugated to the target protein by forming polyubiquitin chain which leads to its recognition by proteasome receptors that in turn binds target protein and degrades it by proteolysis (Morgan, 2007; Wei & Yihong, 2009). Specifically, in *S.cerevisiae*, the glycine residue of distal ubiquitin can be ligated to any of the seven accessible lysine residues in

the proximal ubiquitin, bringing about the arrangement of polyubiquitin chain with particular linkages between ubiquitin moieties (Wei & Yihong, 2009).

1.5.2. E3 enzyme complexes

Degradation of cell cycle regulatory components are essentially performed by two related multisubunit E3 enzyme complexes: SCF (Skp1/cullin/F-box protein) and APC/C (anaphase-promoting complex or cyclosome) (Morgan, 2007; Vodermaier, 2004). The SCF complex controls G1/S and G2/M transition, while APC/C mediates metaphase-anaphase transition by tagging specific proteins with ubiquitin in order to facilitate their degradation (Vodermaier, 2004).

As the name implies, SCF consists of three core subunits: an adaptor protein (Skp1), a structural subunit (Cdc53 in yeast, Cul1 in mammals), and a RING finger protein (Rbx1), plus substrate-binding F-box proteins (FBP) which binds to the Skp1 subunit of the SCF complex, opposite to the ubiquitin that is conjugated to E2 (Feldman et al., 1997; Landry et al., 2012; Morgan, 2007; Ohta et al., 1999; Seol et al., 1999; Skowyra et al., 1997).

In addition to being substrate-binding subunit, FBP confers the target specificity of the SCF complex (Landry et al., 2012). In budding yeast, only 3 (Met30, Grr1, and Cdc4) out of 11 F-box proteins have been shown clearly associated with SCF, while 2 (Grr1 and Cdc4) of them are involved in cell cycle regulation each with a particular set of substrates (Deshaies, 1999; Patton et al., 1998; Reed, 2003). SCF^{Cdc4} is responsible for the degradation of CDK inhibitors Sic1, Far1, and the replication protein Cdc6, while SCF^{Grr1} facilitates degradation of G1/S cyclins (Cln1 and Cln2) and putative Cdc42 effector Gic2 (Drury et al., 1997; Henchoz et al., 1997; Hsiung et al., 2001; Jaquenoud et al., 1998; Mann & Commission, 2015; Patton et al., 1998; Skowyra et al., 1997).

One of the factors behind such substrate specificity is a difference in subcellular localization of SCF complexes and their substrates. Minutely, SCF^{Cdc4} is a nuclear enzyme complex due to a monopartite nuclear localization signal (NLS) comprising 82-85 amino acids in its N-terminal region, while SCF^{Grr1} is found both in nucleus and cytoplasm of the cell keeping the

uncertainty about the existence of NLS or nuclear export signal (NES) in any domain of the enzyme (Blondel, 2000; Dingwall C & Laskey RA, 1991). Alongside, as G1/S cyclins are primarily cytoplasmic they are only accessible to SCF^{Grr1} which makes their degradation Grr1 specific (Landry et al., 2012; Miller & Cross, 2000, 2001). However, despite Sic1 and Far1 are nuclear proteins, their ubiquitination is only facilitated by SCF^{Cdc4} indicating that subcellular localization is not the only factor that influences substrate specificity (Blondel, 2000; Landry et al., 2012; Skowyra et al., 1997).

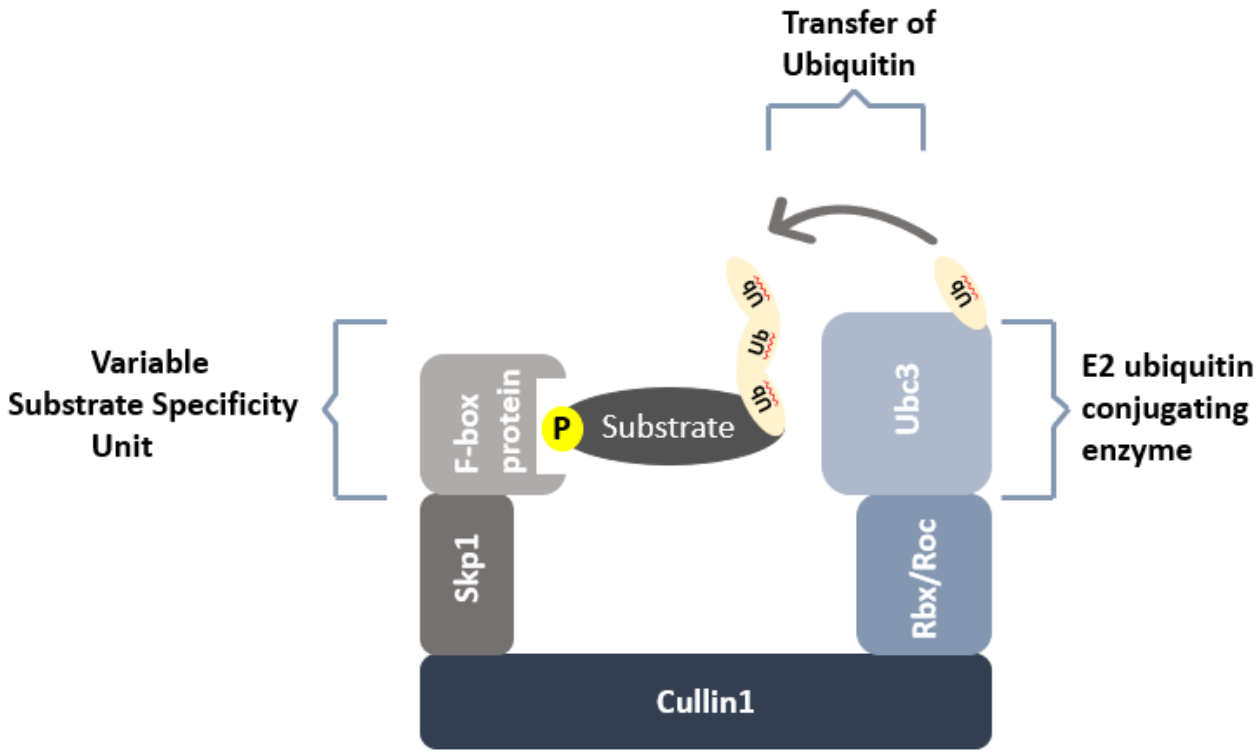

Figure 4. SCF complex. SCF complex is E3 enzyme complex that controls G1/S and G2/M transitions in cell cycle. This enzyme complex consists of three core subunits: an adaptor protein (Skp1), a structural subunit (Cullin 1), and a RING finger protein (Rbx/Roc), plus substrate-binding F-box proteins (FBP) which binds to the Skp1 subunit of the SCF complex, opposite to the ubiquitin that is conjugated to E2 (Ubc3). FBP confers the target specificity of the SCF complex by recognizing specific set of phosphorylated substrates.

One of the requirements to be recognized by FBPs is the post-translational phosphorylation of target proteins. FBPs recognize such phosphorylated epitopes through their distinct phosphorecognition domains: leucine-rich repeat (LRR) domain in Grr1 and WD40 repeat domain in Cdc4 (Hsiung et al., 2001; Landry et al., 2012; Willems et al., 2004). Especially, Hsiung et al., 2001 have extensively studied the LRR domain by analyzing an interaction between SCF^{Grr1} and phosphorylated Cln2. It has been shown that an unusually high number of basic residues on the concave surface of the LRR domain and its carboxy-terminus makes such structure highly positively charged and leads to the recognition of negatively charged phosphorylation epitopes on the phosphorylated Cln2 cyclin (Hsiung et al., 2001; Kishi & Yamao, 1998).

1.5.3. Cln2 phosphodegron

Phosphodegron is a domain of the protein containing all phosphorylation epitopes which mediates degradation of the protein by facilitating its recognition by the SCF enzyme complex (Orlicky et al., 2003). Phosphodegron structure has been further explained by extensive studies on Cln2 phosphodegron.

Cln2 has seven CDC28 phosphorylation sites (T311, T381, S396, T405, S427, T430, S518), while its phosphodegron comprises of PEST element (a sequence rich in proline, aspartate or glutamate, serine, and threonine residues) and four crucial phosphorylation sites S396, T405, S427 and T430 (Berset et al., 2002). The PEST sequence is found in all G1 cyclins and due to its frequent occurrence in the constitutive proteins, it was considered as a potential determinant of protein instability but has yet to be functionally defined (Lanker et al., 1996; Rechsteiner & Rogers, 1996; Berset et al., 2002). It has been shown that deletions in the C- terminus of Cln2 and Cln3 including PEST motif result in a similar phenotype consistent with hyperactivated Cln cyclins, which indicates a partial stabilization of cyclins (Salama et al., 1994; Yaglom et al., 1995). Additional studies on the cell behavior upon introducing several mutations on the PEST and relevant sequences have shown an increase in the stability of cyclin (Lanker et al., 1996; Salama et al., 1994; Yaglom et al., 1995).

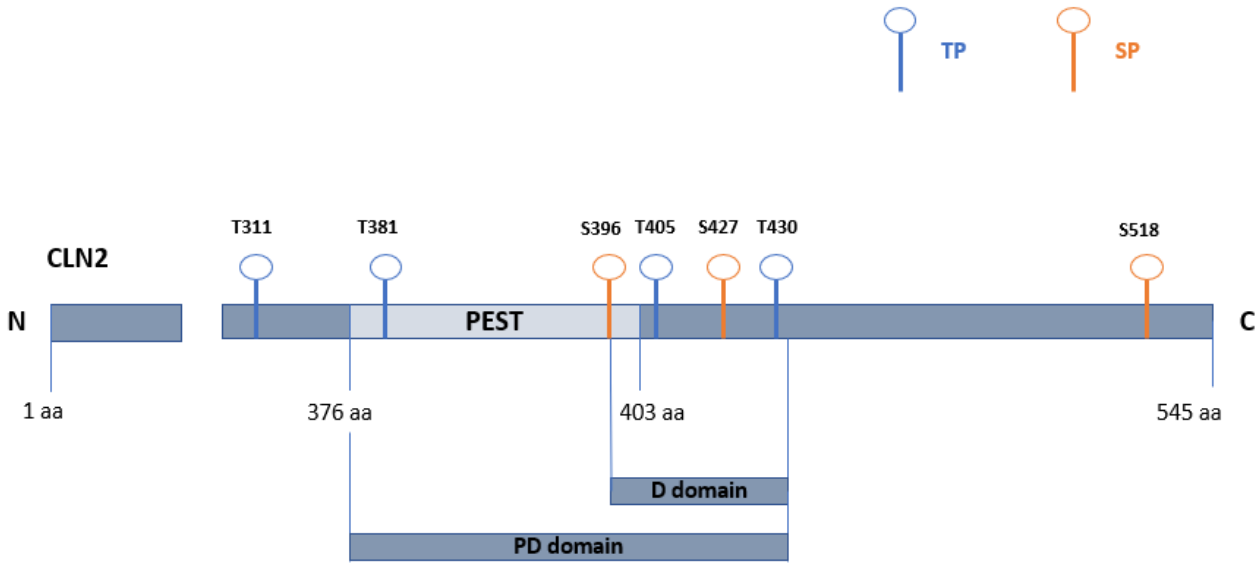

Figure 5. CLN2 C-terminal map. Cln2 C-terminal contains seven CDC28 phosphorylation sites (T311, T381, S396, T405, S427, T430, S518). The terminal is composed of 2 different protein domains, PEST sequence and D domain. The mutation of the phosphorylation sites of PEST sequence causes the partial stabilization of the Cln2, while same mutation on the phosphorylation sites of D domain result in the highly stabilized Cln2 cyclin in the level of seven-site mutant, $Cln2^{4T3S}$. PD domain denotes the region with the phosphorylation sites that affect degradation of Cln2 cyclin.

For example, it has been shown that $Cln2^{S396A}$ and $Cln2^{S427A}$ mutants increase the half-life of cyclin from 8 ± 2.5 min to 11 ± 3 min and 21 ± 2 min respectively, while alanine substitution at both Ser^{396} and Ser^{427} ($Cln2^{S396A, S427A}$) resulted in a rise of half time up to 35 min. Similarly, the deletion of residues from 376 to 514 brings on a highly stable form of Cln2, however, substitution at site 7 does not show any effect on Cln2 stability. According to the cyclin stability in all possible combinations of permutated alanine substitutions of site 2,4, and 6 with site 3 and 5 mutants, it has been interpreted that site 2 mutant slightly but consistently destabilized Cln2. Regarding such interpretation, a particular mutant termed $Cln2^{M46}$, which is composed of mutated phosphorylation sites of 3, 4, 5, and 6 was stabilized into the level that is comparable to that of seven-site mutant, $Cln2^{4T3S}$. Such mutated phosphorylation epitopes are located in a distinct 35 amino acid domain, termed D domain, which overlaps on 9 amino acids with PEST (P) sequence, and the latter result denotes D domain as a determinant for Cln2 instability (Berset et al., 2002; Lanker et al., 1996).

The research on the fusion of several truncated versions of Cln2 C-terminal domain to a stable ΔN-Sic1 reporter has shown that Cln2 phosphodegron might be used as a transferrable domain to facilitate degradation of other proteins through SCF^{Grr1} ubiquitination pathway (Berset et al., 2002; Feldman et al., 1997; Skowyra et al., 1997; Verma et al., 1997). Sic1 is ubiquitinated through the SCF^{Cdc4} enzyme complex whose recognition is mediated by its N-terminal 105 aa and it has been shown that ΔN-Sic1 (aa; 106 to C- terminus) is highly stable protein (Berset et al., 2002).

Accordingly, N terminally truncated Sic1 was fused with following Cln2 domains – $2C^{wt}$, $2C^{M46}$, PD (conjugated PEST and D domains), P and D domains separately as well. $2C^{wt}$ domain grafted ΔN-Sic1 was highly destabilized with the half-life of 18 min, while that of wild type Sic1 is less than 5 min. However, the $2C^{M46}$-ΔN-Sic1 protein was highly stable with the half-life of more than 300 min, similarly, P and D fused proteins showed high stability as well with the half-life of about 90 min and 150 min respectively. Nevertheless, PD-ΔN-Sic1 was heavily destabilized suggesting an identification of the Cln2 domain to accord significant instability to ΔN-Sic1. Coherent with their instability $2C^{wt}$-ΔN-Sic1 and PD-ΔN-Sic1 were highly ubiquitinated while $2C^{M46}$-ΔN-Sic1, P-ΔN-Sic1, and D-ΔN-Sic1 did not show any significant ubiquitination (Berset et al., 2002).

In addition, the coimmunoprecipitation experiments with C terminally 6His tagged Grr1 and Cdc4 have shown that Grr1-6His only coprecipitated with $2C^{wt}$, PD, and surprisingly D fused ΔN-Sic1 proteins, while Cdc4-6His was not able to make an interaction with 2C-ΔN-Sic1 fusions. These all take us to the conclusion that $2C^{wt}$ and PD domains facilitated ΔN-Sic1 truncated protein by switching F-box specificity for Sic1 from Cdc4 to Grr1 (Berset et al., 2002).

2. THE AIMS OF THE THESIS

In recent years, several toolboxes for synthetic biology have been developed for *S.cerevisiae*. These toolboxes include gene expression regulatory modules that provide powerful tools for highly efficient gene expression control. The application of the components of such toolboxes help to improve production of biomolecules or heterologous enzymes. In this work, we are aiming to create a new controllable degron module that can be used to control the level of the desired proteins in order to regulate metabolic dynamics of the budding yeast, *S.cerevisiae*.

It has been previously shown that Cln2 phosphodegron is a transferable protein domain that mediates SCF^{Grr1}specific degradation of conjugated proteins. In addition, from Örd et al., 2020, we know that PxF is a 10 amino acid length Clb3 specific docking motif which means that PxF ligated proteins are predominantly phosphorylated by Clb3-CDC28 complex. In this work, we are aiming to create a controllable protein degradation system by tagging the proteins in the C-terminal with freshly designed Clb3-CDC28 specific degron module, Cln2 phosphodegron – PxF.

The aims of the thesis are:

- To design Clb3-CDC28 specific degron-docking motif: Cln2 phosphodegron-PxF
- To check whether it is possible to mediate degradation of cytosolic-metabolic proteins in *S.cerevisiae* by tagging with a Cln2 phosphodegron – PxF motif module.
- To analyse a degradation efficiency of C-terminally tagged proteins

3. EXPERIMENTAL PART

3.1. MATERIALS AND METHODS

3.1.1. A table of plasmids

Table 1. A list of plasmids used in this work.

Name	Description	Source
pYM17	pTEF – AmpR – natN2	**(Janke et al., 2004)**
pRKI0327	pYM17 GS linker - Sic1 T48+1P S69+2R S80+2R dC 3HA	**This study**
pRKI0328	pYM17 GS linker - Sic1 T48+1P S69A S80A - 3HA k1 - fixed for PCR	**This study**
pRKI0342	pYM17 GS linker 3 HA	**This study**

3.1.2. A table of strains

Table 2. A list of strains used in this work.

Strain	Background	Genotype	Marker	Source
RKI106	DOM0090	B112 transcription factor + pEstr Clb3del130 NES GFP	HIS URA	**Rait Kivi**
RKI0406	RKI106	Cit2 C-terminal degron TTT STST PNF 3HA	HIS URA Nat	**This study**
RKI0418	RKI106	Cit2 C-terminal degron TTT AAAA PNF 3HA	HIS URA Nat	**This study**
RKI0465	RKI106	Cit2 C-terminal 3HA	HIS URA Nat	**This study**
RKI0411	RKI106	Trp2 C-terminal degron TTT STST PNF 3HA	HIS URA Nat	**This study**
RKI0413	RKI106	Trp2 C-terminal degron TTT AAAA PNF 3HA	HIS URA Nat	**This study**
RKI0466	RKI106	Trp2 C-terminal 3HA	HIS URA Nat	**This study**
RKI0421	RKI106	Ade12 C-terminal degron TTT STST PNF 3HA	HIS URA Nat	**This study**
RKI0422	RKI106	Ade12 C-terminal degron TTT AAAA PNF 3HA	HIS URA Nat	**This study**
RKI0464	RKI106	Ade12 C-terminal 3HA	HIS URA Nat	**This study**

3.1.3. A table of primers

Table 3. A list of primers used in this work

Number of the primer in Loog Lab database	**Sequence**
5506	AGA TCT GGC GCG CCC TAC GCA TAA TCG GGT ACA TCG TAC
5649	CAG CTG AAG CTT CGT ACG CTG CAG GTC GAC GGT GGT GGA GGC TCT GGA
5630	ATG GGT TGG TAC CGG CCC CGC AAG AGA AAG CAT GTT GCA TAA AGA AAT TAA ACG TAC GCT GCA GGT CGA C
5631	ACT GTG AAA AGA AAT TAA ATT GAA GTT TGT CAT GGA TGT CCA ACG CCC TAA TCG ATG AAT TCG AGC TCG
5606	TCC TAT TCT ACT GAG AAA TAC AAG GAA TTG GTC AAA AAC ATT GAA AGC AAA CTA CGT ACG CTG CAG GTC GAC
5607	ATG AGG AAA GAA AAA TAT GCA GAG GGG TGT AAA AGT AGG ATG TAA TCC AAC TAA TCG ATG AAT TCG AGC TCG
5626	CAG TAC TAT TGT GCA AGC AGA AGA ATT GTG GGC CGA TAT CGT AGG ATC AGC TCG TAC GCT GCA GGT CGA C
5627	AAA ACT ATA AAA ATG TCG TCT AAG GGG AAA AAA ACA GAG AAT GCC CTT TTT AAT CGA TGA ATT CGA GCT CG

3.1.4. Plasmid construction

In order to create 3 different types of modules (reference to the module scheme figure) we used pYM17 plasmid (Table 1) as a backbone for plasmid construction. pYM17 contains an ampicillin resistance gene used as a selection marker in bacteria and natNT2 gene which behaves as a yeast selectable marker. Tag sequences were designed in Benchling.com and ordered as synthetic DNAs (Integrated DNA Technologies, Belgium).

3.1.4.1. Insert amplification PCR

To introduce 3xGGGGS linker into the 5'-end of the inserts, synthetic DNAs (Supplementary Material) containing 3xHA tags conjugated degron-docking motifs, and just 3xHA tag were amplified by PCR via forward primer (5649) with 3xGGGGS linker, HindIII cutting site and reverse primer (5506) with SgsI cutting site. The volume of the reaction mixture was 50 µL. The mixture was composed of 1x concentration of 5x Phusion HF Buffer (Thermo Fisher Scientific), 250 µM final concentration of 25 mM dNTPs, 0.3 µM final concentration of each forward and reverse primers, and 1 µL of template DNA and 0.5 µL of high-fidelity Phusion DNA Polymerase (Thermo Fisher Scientific). In the final step, the required amount of milli-Q H2O was added to the mixture to complete the volume to 50 µL.

Table 4. PCR program for insert amplification

Step	Temperature	Time	Cycle
Initial Denaturation	98°C	5 minutes	1
Denaturation	98°C	30 seconds	33
Annealing	56°C	25 seconds	
Extension	72°C	50 seconds	
Final Extension	72°C	5 minutes	1
Final Hold	15°C	Until the program is stopped manually	

In the next step prepared mixture was taken into the PCR machine to run the reaction for which the steps have been described in Table 4. The annealing temperature of the reaction has been calculated according to the length and sequential content of the primers via an online software platform, Benchling (www. benchling.com). Extension time has been calculated by accounting the length of the amplicon considering that 30 seconds per kilobase is required for Phusion Polymerase catalyzed reactions.

3.1.4.2. Agarose gel electrophoresis

Once the PCR was done, the reaction sample was stained with 6x DNA Loading Dye (Thermo Fisher Scientific) in a final concentration of 1x and loaded on to 1% Agarose gel (40 mM Tris-acetate with pH 8.3, 1 mM EDTA, 1% agarose, 0.05 µL/µL Atlas ClearSight DNA Stain (BioAtlas)). To assess PCR product sizes, 4 µL of GeneRuler DNA Ladder #1 (Thermo Fisher Scientific) was added onto the gel. To be run for 25 minutes at 170V, the gel was put into the gel electrophoresis machine filled with 1xTAE buffer (40 mM Tris-acetate (pH 8.3), 1 mM EDTA).After electrophoresis picture of the gel was taken under the UV light (280 nm) and the bands with the corresponding size were cut out of the gel and placed in an empty Eppendorf tubes. DNA was purified from the gel piece by FavorPrep™ GEL/PCR Purification Kit (Favorgen) according to the protocol provided by the manufacturer.

3.1.4.3. DNA concentration measurement

The concentration of extracted DNA was measured by NanoDrop 1000 3.8.1 software in NanoDrop 1000 Spectrophotometer (Thermo Fisher). 1,5 µL of each sample was used for measurement. 1,5 µL of elution buffer by FavorPrep™ GEL/PCR Purification Kit (Favorgen) was used for blank measurements.

3.1.4.4. Enzyme restriction

To be ligated to the backbone plasmid, amplified inserts were supposed to be restricted by the corresponding enzymes. The restriction was performed by HindIII/SgsI Termo Fisher's FastDigest™ enzymes. The 30 µL reaction mixture was composed of 1000 ng of amplified insert, 10x FastDigest™ Buffer in a final concentration of 1X, 1 µL of each restriction enzyme, and Milli-Q H2O was added up to mixture volume. The prepared reaction mixture was gently re-suspended by the pipette and subsequently incubated at 37°C heat block for 30 minutes. Reaction was stopped by heating the reaction mixture at 65°C thermostat for 20 minutes. In the next step, the backbone plasmid (pYM17) was restricted to linearize the circular pYM17 vector by HindIII/SgsI Termo

Fisher's FastDigest™ enzymes. The 30 µL reaction mixture was composed of 2 µg of pYM17 backbone plasmid, 10x FastDigest™ Buffer in a final concentration of 1x, 1 µL of each restriction enzyme, 1 µL of FastAP (Thermo Fisher Scientific), and the rest of the mixture was completed with Milli-Q H2O. FastAP is an alkaline phosphatase that catalyzes the removal of the phosphate groups in the sites where the restriction enzymes leave the cut to prevent the re-ligation of the restricted backbone plasmid. The reaction mixture was incubated at 37°C heat block for 40 minutes. The restricted backbone was checked by agarose gel electrophoresis and purified (see section 3.1.4.2), DNA was isolated from the gel piece by FavorPrep™ GEL/PCR Purification Kit (Favorgen) according to the protocol provided by the manufacturer, and the concentration was measured as in section 3.1.4.3.

3.1.4.5. Ligation

After restriction, the vector and insert were ligated together in 10 µL of the reaction mixture. The ligation mixture was composed of a 1x concentration of 10x T4 DNA Ligase Buffer, insert/vector in 3:1 volume ratio, 0.5 µL of T4 DNA Ligase (Thermo Fisher Scientific), and Milli-Q H2O was added up to reaction volume. The prepared mixture was gently suspended by the pipette and incubated at 16°C overnight.

3.1.4.6. Bacterial transformation

After ligation the plasmids were transformed into *E. coli* DH5α competent cells. The bacterial cells were taken out of -80°C freezer and thawed on ice. 50 µL of competent cells were mixed with 2 µL of ligation mixture in the separate Eppendorf tube by gently resuspending and the mixture was chilled on ice for 30 minutes. After incubation, heat shock was applied to the transformation mixture for 45 seconds at 42°C thermostat and chilled on ice for 2 minutes. 500 µL of LB media (5 g/L yeast extract (Formedium), 10 g/L tryptone (BD Biosciences), 10 g/L NaCl) was added to the mixture and incubated for 50 minutes in 220 rpm shaker at 37°C. After incubation, the cells were centrifuged down for a minute at 3300 g. 300 µL of the supernatant was removed and the pellet was resuspended in the rest of the media. In the final step, the cells were plated on LB plates that contained 100 µg/mL ampicillin and incubated for 12-15 hours at 37°C incubator.

3.1.4.7. Plasmid verification

Few bacterial colonies that appeared on ampicillin selection plates were inoculated in glass tubes containing 5 mL of LB media (5 g/L yeast extract (Formedium), 10 g/L tryptone (BD

Biosciences), 10 g/L NaCl) with 100 µg/mL ampicillin. The tubes were incubated for 12-16 hours in 220 rpm shaker at 37°C. After the incubation, the plasmids were extracted from the cultures via FavorPrep™ Plasmid DNA Extraction Mini Kit (Favorgen) according to the protocol provided by the manufacturer. The concentration of the extracted DNA was measured as in section 3.1.3.3. To determine the plasmid containing the right insert, the plasmid was restricted by HindIII and SgsI Termo Fisher's FastDigest™ enzymes. The 20 µL restriction reaction mixture was composed of 1.5 µg of plasmid, 10x FastDigest™ Buffer in a final concentration of 1X, 0.5 µL of each restriction enzyme, and the rest of the mixture was completed with Milli-Q H2O. The reaction mixture was incubated for 20-30 minutes at 37°C heat block. Finally, the reaction mixture of restricted plasmid was analyzed using agarose gel electrophoresis (section 3.1.4.2). 300-500 ng of samples containing appropriately sized insert were sent for sequencing to the Estonian Biocentre core laboratory.

A

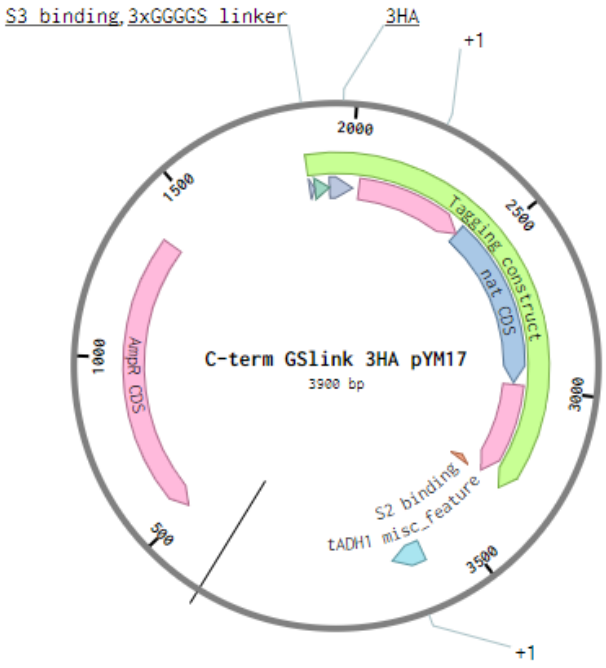

B

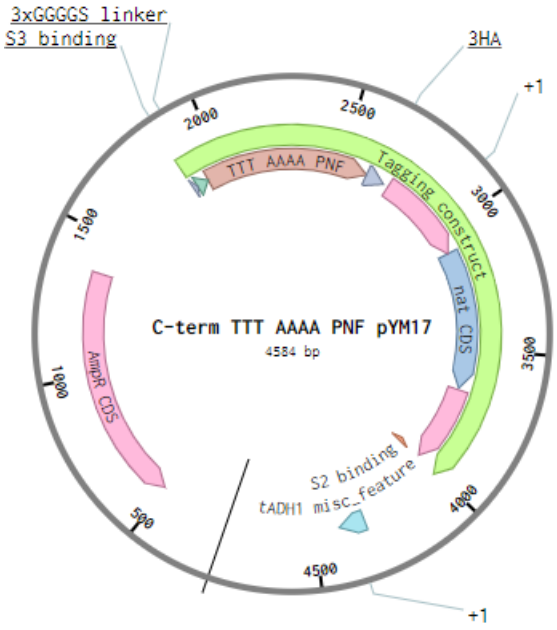

C

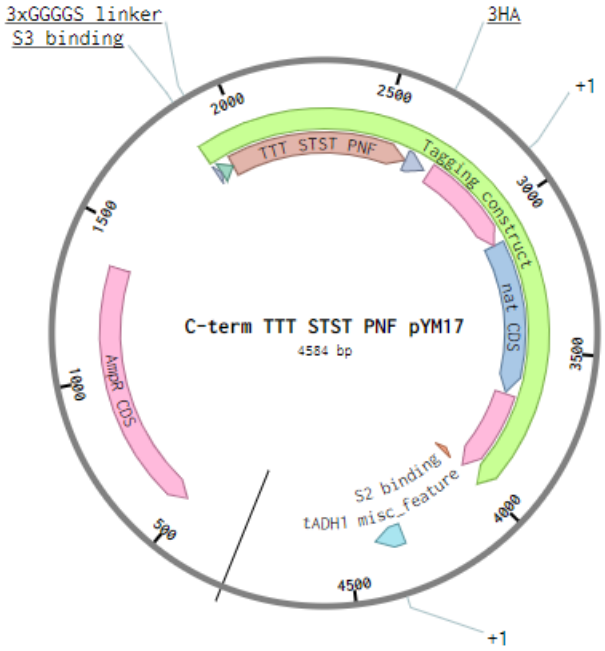

Figure 6. The map of the created plasmids. A) The plasmid containing no degron module. B) The plasmid containing AP degron module. C) The plasmid containing wt degron module.

3.1.5. Amplification of the tagging modules

Three different modules (Figure 7) were amplified from the created plasmids (Figure 6) by 3 different primer pairs with overhangs that introduce homologous ends each specific to the distinct cytoplasmic protein (Protein-primer pair: Ade12-(5626/5627), CIT2-(5606/5607), Trp2-(5630/5631)). The reaction was performed as in section 3.1.3.1 with different PCR program (Table 5), while the samples containing desired amplified DNA were identified and purified as in 3.1.4.2.

Table 5. PCR program for amplification tag amplification

Step	Temperature	Time	Cycle
Initial Denaturation	98°C	5 minutes	1
Denaturation	98°C	10 seconds	36
Annealing	60°C	15 seconds	
Extension	72°C	1 minute 15 seconds	
Final Extension	72°C	10 minutes	1
Final Hold	15°C	Until the program is stopped manually	

3.1.6. Yeast transformation

Amplified tagging modules were transformed in *S.cerevisiae* strain, RKI106 (Table 2) which was obtained from Rait Kivi. The strain was taken from the stock in -80°C fridge by sterile streaking stick and was spread on YPD (10 g/L yeast extract (Formedium), 20 g/L glucose (Oriola), 20 g/L peptone (Formedium)) plate. The plate was incubated overnight at 30°C incubator. The next day, the cells were inoculated in a glass tube containing 5 mL of YPD media. The tube containing inoculated cells was incubated at 30°C shaker for overnight. After incubation, the optical density of the culture was measured by spectrophotometer Ultrospec 10 (Amersham Biosciences) at 600 nm wavelength (0.1 of OD600 = $1*10^6$ cells/mL, for the calibration 1 mL of

growth media was used). The culture was diluted in YPD media to reach the final OD of 0.2 in the final volume of 50 mL, an Erlenmeyer flask. The flasks were incubated at 30°C shaker until the cultures reached OD of 0.6-0.8.

The culture was transferred from the flask to a 50 mL falcon tube and was centrifuged for a minute at 1811 g. The supernatant was discarded, the pellet was re-suspended in 1 mL of sterile P.L.I buffer (100mM of lithium acetate (LiAc) in 0.5xTE buffer (5 mM Tris-HCl (pH 8), 0.5 mM EDTA (pH 8)) and the mixture was centrifuged for a minute at 1200 g.. Then the supernatant was removed, and the pellet was re-suspended in two times the cell volume of P.L.I buffer. The mixture was incubated at room temperature for 10 minutes.

Meanwhile, Salmon Sperm DNA (SSDNA) was incubated at 100°C for 10 minutes and chilled on the ice. After the chilling, the 40 µL of the purified PCR product was mixed with 10 µL of SSDNA in a separate Eppendorf tube, and 100 µL of yeast competent cells were added on the mixture. Subsequently, 700 µL of sterile PEG/LiAc (100mM lithium acetate, 10 mM Tris-HCl (pH 8), 1 mM EDTA, 40% PEG 3350) solution and 48 µL of DMSO were added into the mixture which was followed by slow re-suspension by the pipette. The mixture was incubated at 42°C thermostat for 40 minutes and the tube was chilled on the ice for 2 minutes. Afterward, the mixture was centrifuged for a minute at 3300 g, the supernatant was removed, and the cell pellet was re-suspended in 1 mL of sterile 1x TE buffer (10 mM Tris-HCl (pH 8), 1 mM EDTA). Then the mixture was centrifuged at 1000 g for 2 minutes, the supernatant was removed, and the cell pellet was re-suspended in 200 µL of 1x TE buffer (10 mM Tris-HCl (pH 8), 1 mM EDTA). The cells were plated on YPD (10 g/L yeast extract (Formedium), 20 g/L glucose (Oriola), 20 g/L peptone (Formedium)) plate and were incubated at room temperature for overnight.

3.1.7. Replica plating

After the overnight incubation, transformed yeast cells were transferred from YPD plate to the Nourseothricin (clonNAT) (10 g/L yeast extract (Formedium), 20 g/L glucose (Oriola), 20 g/L peptone (Formedium), 100 µg/mL clonNAT) selection pates by a replica plating technique.

In the first step, the colonies were replicated on the velveteen by pressing down the media containing side of the YPD plates on the sterile velveteen covered metal block. In the next stage, the colonies were imprinted on the clonNAT selection plates, by pressing down the selective media

containing side of the clonNAT plates on the colonies replicated velveteen covered metal block. The clonNAT selective plates were incubated at 30°C incubator for 2 days.

3.1.8. Identification of successfully tagged colonies

3.1.8.1. Sample Preparation

The day before the sample preparation the colonies were streaked to the new clonNAT plates and were incubated at 30°C incubator overnight. The next day, the cells were inoculated by the sterile streaking stick in a glass tube containing 5 mL YPD media and the cultures were incubated at 30°C shaker for overnight. After 12-16 hours, the optical density of the cultures was measured by spectrophotometer Ultrospec 10 (Amersham Biosciences) at 600 nm wavelength (0.1 of OD600 = $1*10^6$ cells/mL, for the blank measurement 1 mL of growth media was used). The cultures were diluted in YPD media to reach a final OD of 0.2 in the final volume of 5 mL, in a glass tube. The cultures were incubated at 30°C shaker until the culture reached OD of 0.6-0.8. Then the cultures were transferred to the 15 mL tubes and the cells were collected by the centrifuge at 1811 g for a minute, supernatant was removed, and cells were immediately frozen in liquid nitrogen. After freezing, the tubes were stored in -80°C freezer.

3.1.8.2. Western Blotting

The tubes were taken from -80°C freezer and were thawed on ice. 200 µL of the glass bead was added into the separate Eppendorf tube. Cell pellet was resuspended in 200 µL of urea lysis buffer (20 mM Tris (pH 7.4), 8 M Urea, 2M Thiourea, 4% CHAPS, 1% DTT, 50 mM NaF, 89 mM BGP, 1 mM Na3VC4) and the mixture was added into the Eppendorf tube containing 200 µL of the glass bead. Afterward, the cells were disrupted in FastPrep-24 bead beater (MB Biomedicals) at 4 meters/second for 40 seconds.

After breaking the cell walls, the hole was made in the bottom of the tube by a heated needle, thereafter the tube was put into the separate Eppendorf tube and a quick spin-down was applied to transfer the lysate into the new Eppendorf tube. In the next step, the old tube was thrown away and the tube containing lysate was centrifuged at maximum speed for 10 minutes by Centrifuge 5415 D from eppendorf. Subsequently, 10 µL of supernatant was stained with 1x final concentration of 3x SDS buffer (375 mM Tris-HCl 9% SDS 50% Glycerol 0.03% Bromophenol blue) and loaded onto the 10% acrylamide gel (separating gel: 0.375 M Tris-HCl (pH 8,8), 10% acrylamide [29:1 acrylamide:bis-acrylamide], 0,1% SDS; stacking gel: 0.125M Tris-HCl (pH 6,8),

5% acrylamide [29:1 acrylamide:bis-acrylamide], 0,1% SDS) along with 1.5 µL of PageRuler™ Prestained Protein Ladder loaded with 5 µL of 3x SDS buffer.

Proteins were separated on the gel by running SDS-PAGE (sodium dodecyl sulfate-polyacrylamide gel electrophoresis) for 50 minutes at 15 mA. Once the running was finished, the gel was blotted in the Semi-Dry buffer (25 mM Tris-HCl, 192 mM glycine, 0,1% SDSI also lack its mix) for 15 minutes. Meanwhile, 4 layers of the filter papers (Blotting-Papier MN 827 B, Macherey-Nagel, Germany) and a 0.45 µm nitrocellulose blotting membrane (Amersham, Germany) were cut in the same size as the gel is. Afterward, the filter papers and nitrocellulose membrane were soaked in the Semi-Dry buffer as well till 15 minutes were done. In the next step, the so-called sandwich (from bottom to top, 2 layers of filter paper – nitrocellulose membrane – gel – 2 filter paper) was prepared and the transfer of the proteins from the gel onto the membrane was mediated by running the sandwich for an hour using the standard semi-dry transfer program in Pierce G2 Fast Blotter (Thermo Scientific).

After transfer, the membrane was kept in the blocking solution (5% milk powder, 1x TBS-T buffer (20 mM Tris-HCl, 150 mM NaCl, 0.1% Tween20)) for an hour at room temperature or overnight at 4 C on a tilting shaker. Once the blocking finished, the membrane was transferred and incubated in the primary antibody solution (3% milk powder, 1x TBS-T buffer (20 mM Tris, 150 mM NaCl, 0.1% Tween20), 1:500 dilution of mouse anti-HA antibody (Biolegend), 0.03% N_3Na) at room temperature for 30 minutes on tilting shaker. Latterly, the membrane was washed in 1x TBS-T buffer firstly for 15 minutes, then 2 times for 5 minutes. After washing, the membrane was incubated in the secondary antibody solution (3% milk powder, 1x TBS-T (20 mM Tris-HCl, 150 mM NaCl, 0.1% Tween20), 1:7500 dilution of goat anti-mouse HRP-conjugated antibody (LabAs)) at room temperature for 30 minutes on tilting shaker. Afterward, the membrane was washed in 1x TBS-T buffer first for 15 minutes, then for 3 sequential 5 minutes.

In the next step, to visualize the protein bands on the film the surface of the membrane was completely covered within a 1:1 ratio prepared SuperSignal™ West Pico PLUS Chemiluminescent Substrate (Thermo Fisher Scientific) solution and was placed between cellophane layers.

In the last step, the membrane was exposed to autoradiography film (AGFA Medical X-ray film blue, Belgium) in a dark setting for 20 seconds to 10 minutes (depending on the protein expression level). Afterward, the film was popped into the G150 developer (AGFA) for 1 minute,

followed by 15 seconds of drying. Subsequently, the film was washed in water for 10 seconds, followed by 15 seconds drying. Latterly, the film was kept in the G354 fixer (AGFA) for 20 seconds, followed by 20 seconds drying and washed with distilled water. The bands of PageRuler™ Prestained Protein Ladder were marked on the dried film.

3.1.9. Stock preparation

Successfully tagged colonies were taken from clonNAT selection plates and were inoculated in a separate tube containing 1 mL of 15% glycerol solution in YPD media. Afterward, the tube was vortexed and put into a -80°C fridge.

3.1.10. Protein degradation analysis

3.1.10.1. Sample Preparation

The day before the sample preparation the cells were streaked from the stock into the clonNAT selection plates and were incubated at 30°C heat block for overnight. The next day, the cells were inoculated by the sterile streaking stick in a glass tube containing 5 mL YPD media, and the culture was incubated at 30°C shaker for overnight. In the morning, the optical density of the culture was measured by spectrophotometer Ultrospec 10 (Amersham Biosciences) at 600 nm wavelength (0.1 of OD600 = $1*10^6$ cells/mL, for the blank measurement 1 mL of growth media was used). After the proper calculations were done the culture was diluted in YPD media to reach a final OD of 0.2 in the final volume of 5 mL, in a glass tube. The culture was incubated at 30°C shaker till the culture reached OD of 0.6-0.8. Afterward, the culture was collected and divided into half in two separate glass tubes. To induce the degradation of the degron module tagged proteins by the expression of NES-Clb3Δ130, 10 mM of estradiol was added to one of the cell cultures in a final concentration of 1 µM, while another one was left uninduced. Then the cultures were incubated at 30°C shaker for 3 hours. Once the incubation was done, the culture was transferred to the 15 mL tubes, the cells were collected by the centrifuge at 1811 g for a minute, supernatant was thrown away and the cell pellets were promptly frozen in liquid nitrogen.

3.1.10.2. Western Blotting

Western Blotting was performed in the same procedure as it has been mentioned in section 3.1.7.2 with few modifications.

The first modification was that before loading on the gel, the protein concentration of the lysates was measured by Bradford assay (section 3.1.11) and after the proper calculations the protein concentration of all the samples was equalized to avoid false-positive results.

The next modification has been done in the image developing step. Instead of developing the image on the film, the signal analysis of the protein levels was performed in LI-COR Image Studio 4.0 Software.

3.1.11. Bradford Assay

2 µL of lysate was gently re-suspended in 200 µL of 5 times diluted Pierce™ Coomassie Plus (Bradford) Assay Reagent (Thermo Scientific) solution on the 96-well microplate and the measurement was taken by Magellan™ microplate reader software (Tecan).

3.1.12. Signal Intensity Analysis

The analysis of the protein levels was performed according to the the Western Blotting results of 3 different modules conjugated cytosolic-metabolic proteins. The experiments were duplicated for 3 times and Figure 1 illustrates the results from a set of the experiments. The signal intensity of the bands was measured in LI-COR Image Studio 4.0 Software and to obtain the mathematical model of the results, the bar chart diagrams were made in Excel 2016. As a protein level of each construct the mean value of the 3 experimental results were taken, while the error value was calculated according to the Formula 1.

Formula 1: Error value calculation

n: Number of the experiments

Mean: $(Signal\ intensity\ 1 + Signal\ intensity\ 2 + Signal\ intensity\ 3)/n$

STDEV: standard deviation function

$$Error\ value = \frac{STDEV(Mean)}{\sqrt{n}}$$

3.2. RESULTS

In order to create a controllable degradation system, Clb3-CDC28 specific degron module was designed (Figure 7). The degron module (272 amino acids, 29 kDa) is composed of 6 different subparts: 3x GGGGS linker, intrinsically disordered region containing 44 amino acids of Sic1 (Sic1 (1-44)), Cln2_D domain, 2x PnF docking motif, and the domain containing Sic1 residues from the position 120 to 215 (Sic1 (120-215)), and 3xHA tag (Figure 7, "wt degron"). 3x GGGGS linker is a motif containing 3 repeats of Glycine-Glycine-Glycine-Glycine-Serine sequence that provide additional flexibility between the protein and the fused degron tag. Sic1 (1-44) contains 3 threonine residues (T2, T5, T33) that behave as Cks1 priming site to facilitate effective multisite phosphorylation by CDC28 (Loog, 2011). Cln2_D domain is a degron motif containing four CDC28 phosphorylation sites (S48, T57, S79, T82) whose phosphorylation leads to the recognition of the protein by SCF ubiquitin-ligase complex to drive its degradation by proteasome (Berset et al., 2002). 2x PnF is a Clb3 specific docking motif that mediates a predominant phosphorylation of the target protein by Clb3-CDC28 complex (Örd et al., 2020). Sic1 (120-215) domain allows the degron module to mimic Sic1 non-inhibitory C-terminal tail. 3x HA tag is part of the human influenza hemagglutinin (HA) protein that can be detected with HA-specific antibodies in Western Blotting.

Besides Clb3-CDC28 specific degron module, 2 different tagging modules were used as controls in these experiments. The 1st control module is a mutant degron module (Figure 7, "AP degron") at which the phosphorylation sites of degron motif were substituted with alanine residues to prevent the phosphorylation at Cln2_degron domain which hinders the degradation of the proteins. 2nd control module is consisting of just 3x GGGGS linker conjugated 3x HA tag (Figure 7, "no degron") which was used to show regular protein level.

As the main idea to use a new controllable degron module is to control the degradation level of the desired proteins to regulate metabolic dynamics of the *S.cerevisiae*, in this work we decided to check the effectiveness of the degron module on 3 different cytoplasmic-metabolic proteins (Table 6).

In order to check the inducability of the system the experiments were conducted by tagging metabolic enzymes in the strain RKI106 (Table 1). The reason behind the preference on the use of this strain is the presence of NES-Clb3Δ130 sequence under the expression of estradiol inducible

LexA promoter. In this sequence, NES is standing for a nuclear export signal which is a target peptide containing four hydrophobic amino acids that facilitates the transport of expressed Clb3Δ130 from the nucleus to the cytoplasm via nuclear pores by using the nuclear transport system (Xu et al., 2012). Clb3Δ130 denotes the deletion in the N-terminus of the Clb3 cyclin which prevents the degradation of the cyclin by APC/C E3 enzyme complex and leads to accumulation of Clb3-CDC28 complex in the cytoplasm. The presence of LexA promoter results in controllable expression of NES-Clb3Δ130 which can be induced by estradiol (Ottoz et al., 2014). Protein degradation experiments were conducted in 2 different states: expressed and unexpressed NES-Clb3Δ130.

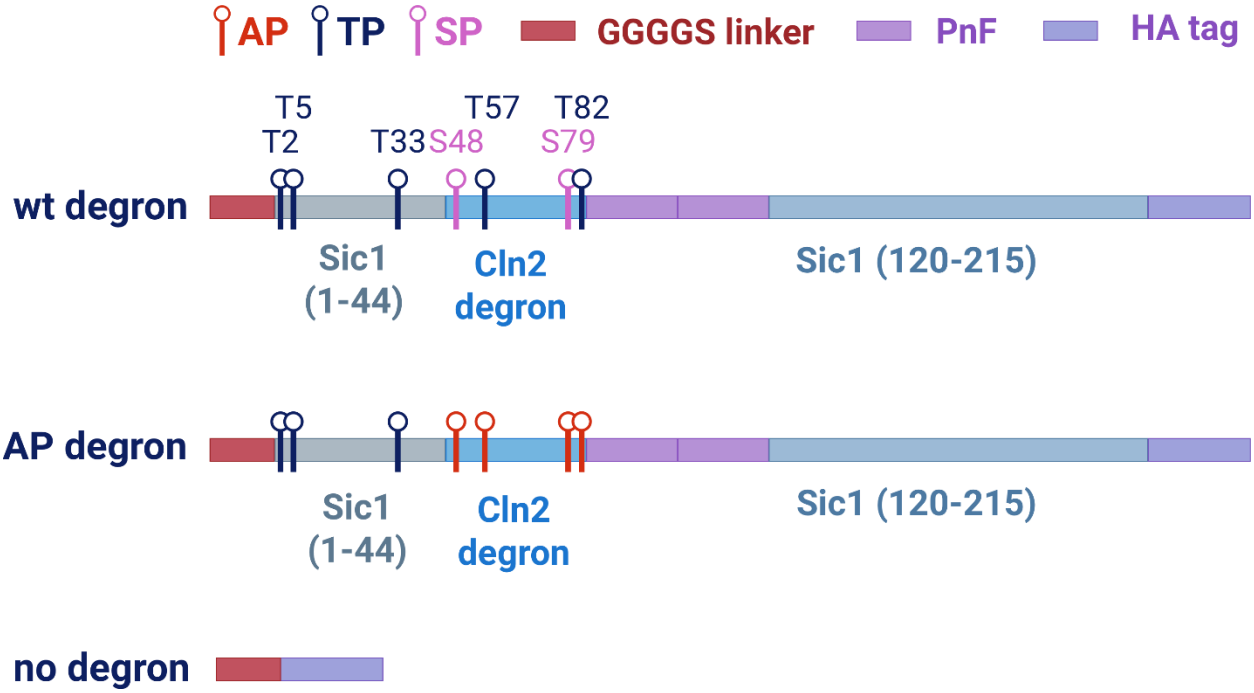

Figure 7. The diagram illustrates the maps of Clb3-CDC28 specific wt degron module and 2 control tagging modules: AP degron and no degron modules. TP stands for threonine phosphorylation residue, SP stands for serine phosphorylation residue, while AP stands for alanine substituted phosphorylation residue.

Table 6. The list of proteins used in this work

Protein	Function	Molecular Weight (kDa)	Median Abundance (Molecules/Cell)*
Ade12	Adenylosuccinate synthase involved in purine nucleotide biosynthesis; localized to the cytoplasm, also binds to the DNA replication origin	48.3	5839 +/- 3065
CIT2	Citrate synthase that catalyzes the formation of citrate from acetyl-CoA and oxaloacetate; localizes to cytoplasm, mitochondria, and peroxisomes	51.4	24307 +/- 11970
Trp2	Anthranilate synthase involved in tryptophan biosynthesis; catalyzes the conversion of chorismate to anthranilate; subunit of the anthranilate synthase complex	56.7	16428 +/- 6426

***** data from Saccharomyces Genome Database (SGD)

3.2.1. Protein level analysis

The abundance of the tagging modules conjugated proteins were obtained based on the signal intensity analysis (3.1.12) of Western Blotting results (Figure 8). The obtained results have been presented in Figure 9. The figure represents the protein levels of degron tagged Ade12, CIT2, and Trp2 in presence or absence of NES-Clb3Δ130. It can be seen from the figure that all proteins tagged with wt degron showed decreased protein levels in samples with induced NES-Clb3Δ130.

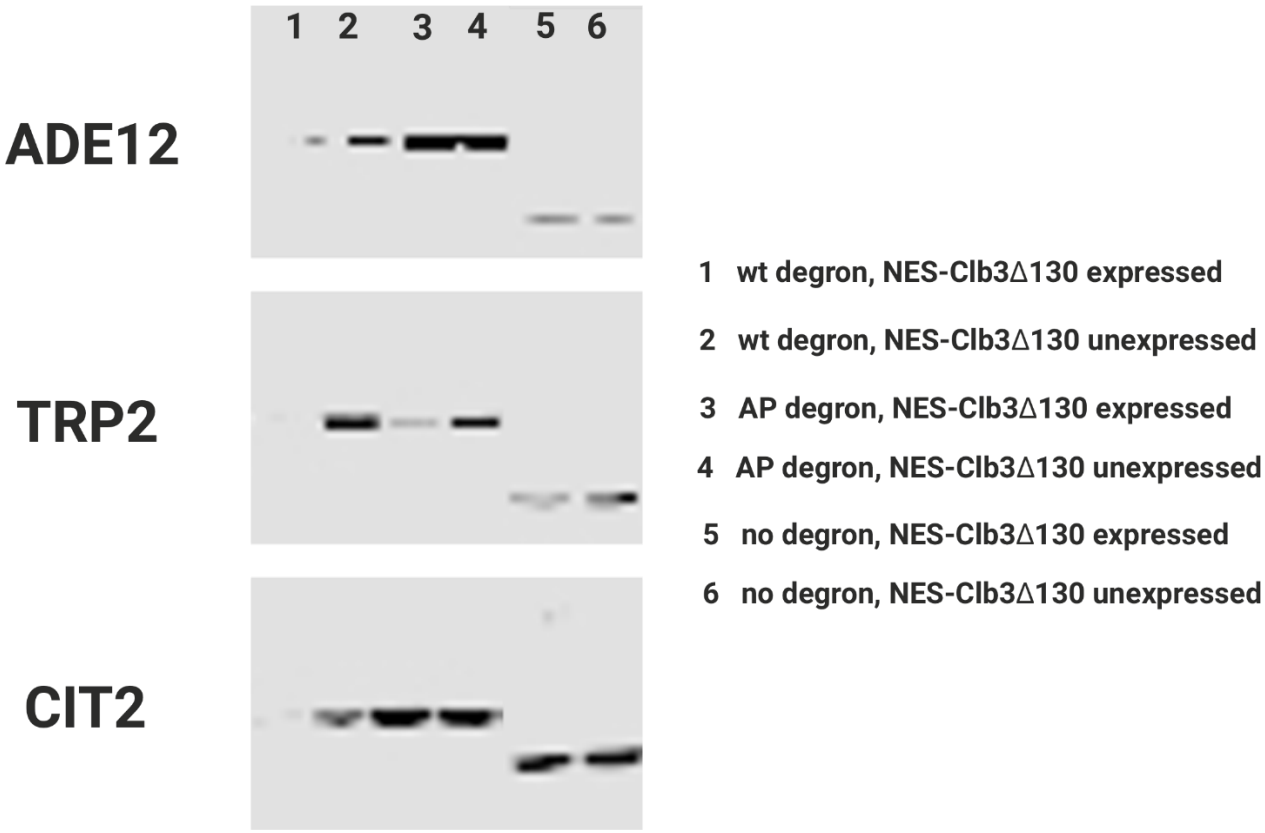

Figure 8. The figure illustrates Western Blotting results for Ade12, CIT2, and Trp2 cytosolic-metabolic proteins.

3.2.2. The Clb3-CDC28 induces the degradation of wt degron tagged protein

The degradation efficiency of wt degron tagged proteins was measured and compared to that of control tagging modules conjugated proteins (Figure 10 A, B). The figure illustrates the change in the protein levels of module tagged cytoplasmic-metabolic proteins by comparison of differently tagged proteins with induced and uninduced Clb3 expression. In case of wt degron conjugation this ratio had the narrowest range for Ade12, CIT2, and Trp2 with the proportion of 0.3, 0.05, and 0.19 respectively. At the same time, it was observed that in case of Trp2 and Ade12, AP degron and no degron modules conjugated proteins showed almost no change in Clb3 expression by keeping the proportion around 1.0, except for CIT2. This data shows that the phosphorylation of S48 T57 S79 T82 residues in Cln2 degron domain is the degradation driving factor of the degron module and the low levels of ratios indicates that this phosphorylation was predominantly performed by Clb3-CDC28 complex.

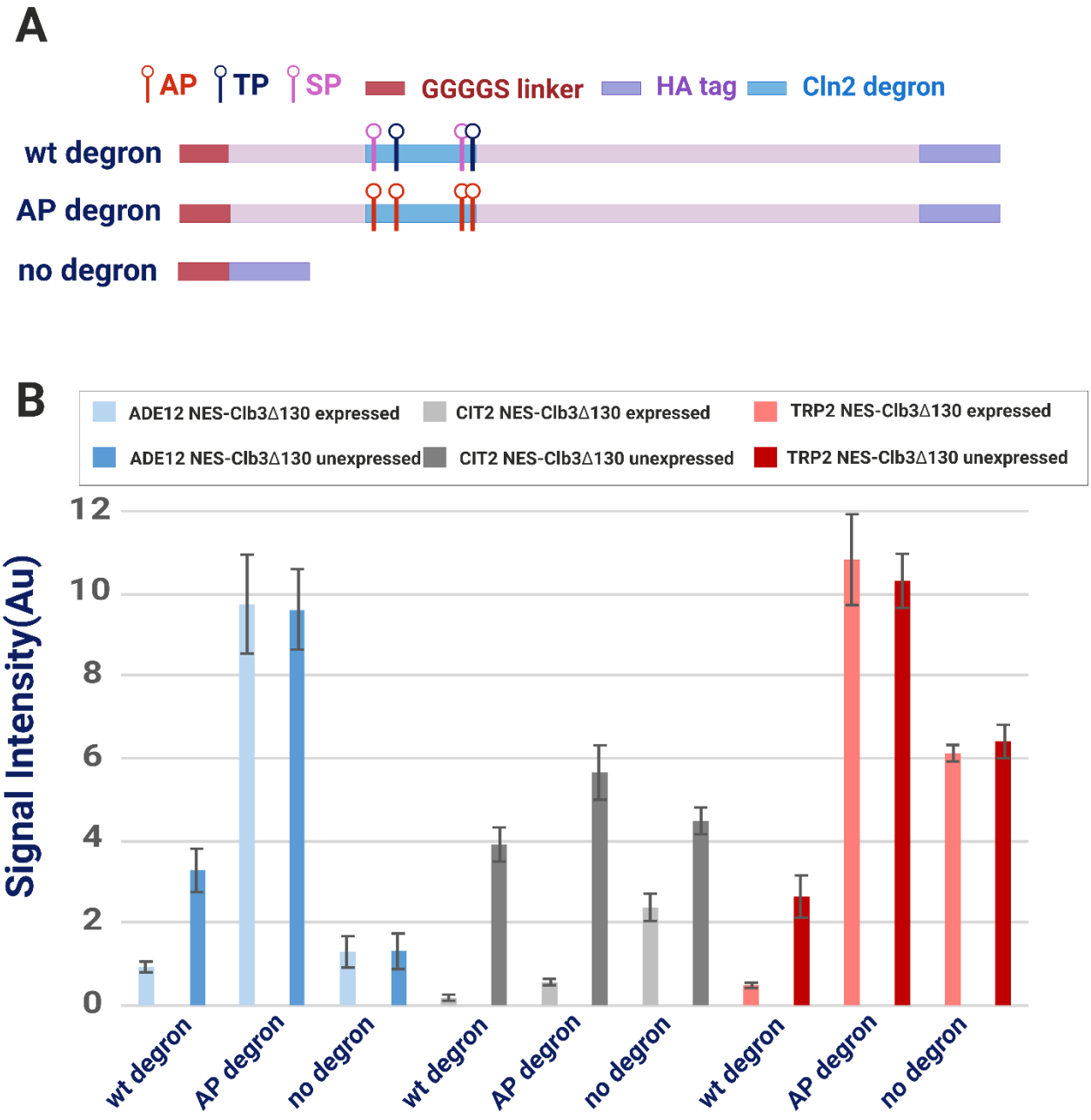

Figure 9. A) The diagram illustrates the simplified maps of Clb3-CDC28 specific wt degron module and 2 control tagging modules: AP degron and no degron modules. TP stands for threonine phosphorylation residue, SP stands for serine phosphorylation residue, while AP stands for alanine substituted phosphorylation residue. B) The bar chart depicts the signal intensities or protein levels of 3 different tagging modules conjugated cytosolic-metabolic proteins in expressed and unexpressed NES-Clb3Δ130 states. The error bars are ±SEM.

However, CIT2 showed an unexpected, interesting behavior regarding the proportion values in AP degron and no degron modules conjugation. Both tagging modules conjugated proteins showed a distinguishable difference in two different states like wt degron conjugation. While wt degron module conjugated protein showed the highest degradation level of the three proteins (0.05), differently from others, the AP degron module conjugated CIT2 had a proportion around 0.1 and no degron module conjugated one showed a ratio of 0.55. Consequently, no matter what tagging module, conjugated CIT2 had a decreased protein level in Clb3 expression. In conclusion, it seems as there is indirect CIT2 regulatory pathway that enhances the degradation of the protein in case of Clb3 overexpression and this result shows that the system is not perfectly orthogonal.

3.2.3. The degradation efficiency is inversely proportional to the median abundance of the protein

From the results it is possible to say that there is a relationship between the degradation efficiency of wt degron and median abundance of the protein (Figure 11). It was observed that Ade12 had the least degradation efficiency with a value of 0.3 while it has the highest median abundance among these 3 proteins. In comparison, the protein with the lowest median abundance, CIT2 showed the highest degradation efficiency with an approximate value of 0.05. Meanwhile, Trp2 showed a degradation efficiency in the middle of the range with an approximate value of 0.19 and it does correspond to its median abundance which is in the middle of the range as well. This data shows that the protein with the least median abundance has the highest degradation efficiency whether, the one with the highest median abundance has the least degradation efficiency. In conclusion, the degradation efficiency of the wt degron is inversely proportional to the median abundance of the protein.

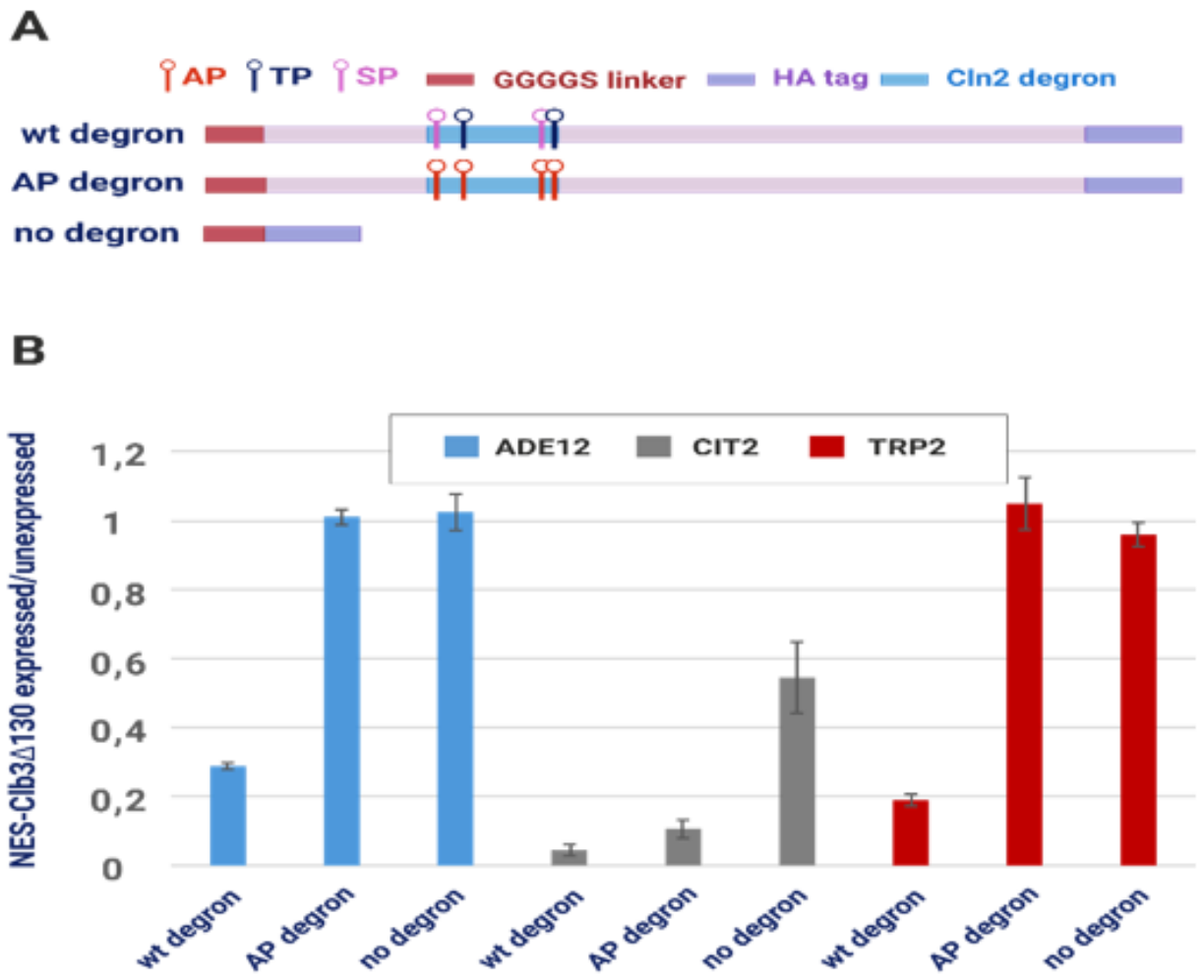

Figure 10. A) The diagram illustrates the simplified maps of Clb3-CDC28 specific wt degron module and 2 control tagging modules: AP degron and no degron modules. TP stands for threonine phosphorylation residue, SP stands for serine phosphorylation residue, while AP stands for alanine substituted phosphorylation residue. B) The bar chart depicts the protein level difference in 2 different states: NES-Clb3Δ130 expressed to NES-Clb3Δ130 unexpressed for 3 different tagging modules conjugated Ade12, CIT2, and Trp2. The error bars are ±SEM.

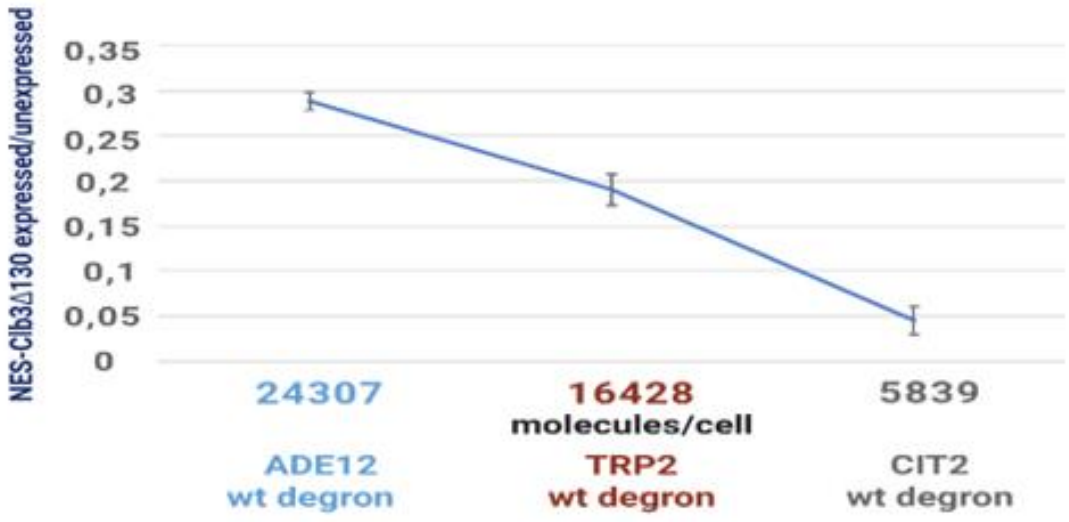

Figure 11. The linear graph describes the relation of wt degron degradation efficiency to the median abundance of the cytosolic-metabolic proteins. As a degradation efficiency the proportion value of wt degron module conjugated cytosolic-metabolic protein was taken from Figure 10 B. The error bars are ±SEM.

3.2.4. The system is not orthogonal and AP degron module conjugation results in the higher stabilized proteins

The abundance of the tagging modules conjugated proteins were compared to each other in unexpressed NES-Clb3Δ130 state (Figure 12 A, B) and the results were presented as proportions. It was observed that wt degron/AP degron value was less than 1 for all proteins, as it showed an approximate proportion of 0.35, 0.7, and 0.3 for Ade12, CIT2, and Trp2 respectively. This data shows that the system is not perfectly controllable and NES-Clb3Δ130 expression is not the only factor that has an effect on the levels of wt degron conjugated proteins.

The wt degron/no degron value were calculated in order to compare the NES-Clb3Δ130 expression independent protein levels. The results showed that the protein level of wt degron conjugated Ade12 was almost 3 times higher than that of no degron module conjugated proteins. At the same time this value was less than 1 for CIT2 and Trp2 proteins with an approximate value of 0.9 and 0.4 respectively, meaning higher stability for proteins without degron tag. This data shows that tagging could have either stabilizing or unstabilizing effect on proteins regardless phosphorylation.

In order to check the effect of the AP degron module on the abundance of the conjugated proteins the AP degron/no degron value of the proteins were analyzed. It was displayed that such value is higher than 1 for all 3 metabolic-cytoplasmic proteins while it was extremely high for Ade12 with an approximate value of 7. In comparison to that of Ade12, for CIT2 and Trp2, this value was around 1.3 and 1.6 respectively. This fact indicates that AP degron module increases the stability by enhancing the expression or hindering the degradation of conjugated proteins.

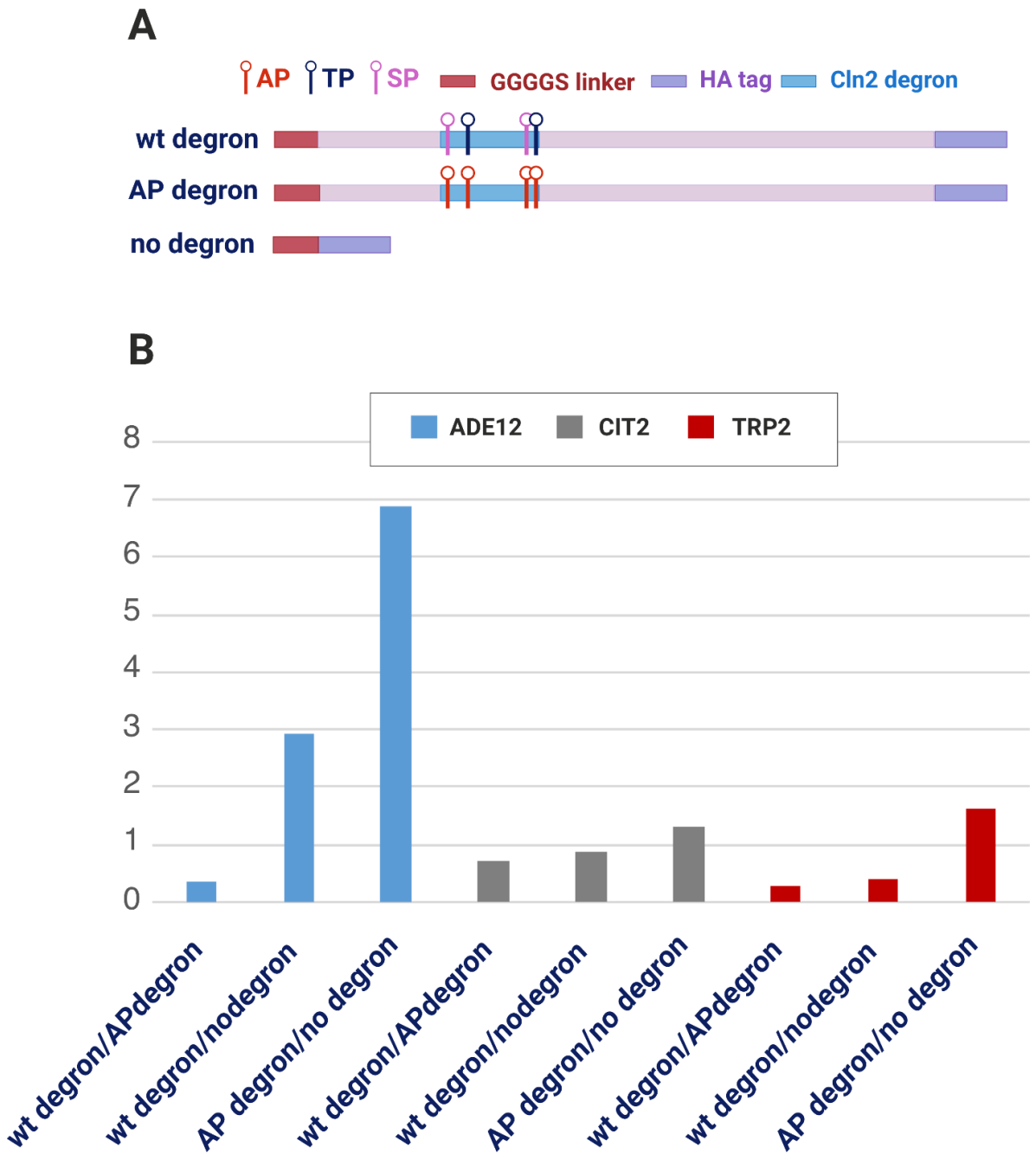

Figure 12. A) The diagram illustrates the simplified maps of Clb3-CDC28 specific wt degron module and 2 control tagging modules: AP degron and no degron modules. TP stands for threonine phosphorylation residue, SP stands for serine phosphorylation residue, while AP stands for alanine substituted phosphorylation residue. B) The bar chart depicts the protein level difference in different tagging modules conjugated proteins in the state of unexpressed NES-Clb3Δ130.

3.3. DISCUSSION

In this work, we studied a Clb3-CDC28 specific degron module which can be used as a synthetic biology tool in order to create a controllable protein degradation system. As the main idea to use a controllable degron module is to control the degradation level of the desired metabolic proteins to regulate metabolic dynamics of the *S.cerevisiae*, the study of the degron module analysis was conducted on the 3 different cytosolic-metabolic proteins: Ade12, CIT2, and Trp2.

In this study it was shown that the degradation of the C-terminal degron module conjugated proteins is mediated by the phosphorylation of the S48 T57 S79 S82 phosphorylation residues in Cln2 degron domain. Also, the experiments that were conducted in presence of NES-Clb3Δ130 expression proved that this phosphorylation is predominantly performed by Clb3-CDC28 complex which makes the degradation controllable. This fact makes the degron module a promising tool to be used in synthetic biology to direct the metabolic dynamics of the host organism.

However, samples with unexpressed NES-Clb3Δ130 showed that NES-Clb3Δ130 expression is not the only factor that drives the degradation of degron module tagged proteins (Figure 11 A, B). As Clb3 is localized to both nucleus and cytoplasm, it could be assumed that the leakage in the degradation of the degron module conjugated proteins is due to the regular expression of Clb3 in the absence of NES-Clb3Δ130 expression. In order to test this hypothesis, we are planning to repeat the experiments in ΔClb3, NES-Clb3Δ130 strain.

During the experiments, tagging modules conjugated CIT2 protein showed an unexpected, interesting behavior. The results indicated that in the state of NES-Clb3Δ130 expression the protein level of CIT2 drops independently from the tagging module it has been conjugated to. It is assumed that this strange behavior is facilitated by indirect CIT2 regulatory pathway activated by Clb3 overexpression, as there is only one potential Cdc20 phosphorylation site in Cit2 protein sequence. This data proves that the system is not perfectly orthogonal, and this concept requires further investigation.

In addition, AP degron module also showed an interesting characteristic in case of the protein instability. The comparison in the protein level of AP degron module conjugated Ade12, CIT2, and Trp2 to that of no degron module tagged ones unveiled that the AP degron module increases the stability of the proteins, especially for Ade12. The reason behind such moderation

can be enhancement of the expression or impedance of degradation of the protein and to check both assumptions the study regarding such case should be furtherly conducted. Another explanation would be that the long unstructured tail of degron modules facilitates better availability of HA antibody epitopes so that the western blotting signals are stronger.

In this study it was also shown that the degradation efficiency of degron module is inversely proportional to the median abundance of the protein it is tagged to. This shows that the degron modules have different efficiency depending on the protein expression which could be imortan when redesigning metabolic pathways in the future.

Regarding the future, we are aiming to conduct the same studies for conjugation of the degron module in N-terminus of the cytosolic-metabolic proteins to check whether the degradation is dependent on the terminal of the protein it is tagged to. In addition, we are planning to design and analyze several truncated versions of the degron module in order to reach the highly effective degron module in the most optimal truncated state.

SUMMARY

Synthetic Biology is recently emerging multidisciplinary field which is seeking out the new biological parts that can be used in the bioengineering of the organisms. In the recent time, there has been a huge enlargement in synthetic biology toolboxes including degron modules that provide powerful tools for highly efficient protein degradation control. The usage of the components of such toolboxes aids to enhance the production of biomolecules or heterologous enzymes. In this work, we designed a Clb3-CDC28 specific degron module that can be used to create a controllable protein degradation system in order to direct the metabolic dynamics of the budding yeast, *S.cerevisiae*. As the main idea to use a controllable degron module is to control the degradation level of the desired metabolic proteins to regulate metabolic dynamics of the *S.cerevisiae,* the study of the Clb3-CDC28 specific degron module analysis was conducted on the 3 different cytosolic-metabolic proteins: Ade12, CIT2, and Trp2.

The results showed that the phosphorylation of four CDC28 target sites (S48 T57 S79 S82) in Cln2 degron domain is the factor that drives the degradation of degron module conjugated proteins, and this phosphorylation is predominantly carried out by Clb3-CDC28 complex which makes the protein degradation controllable.

Nevertheless, in the state of unexpressed NES-Clb3Δ130, a low wt degron/AP degron proportion value depicted that the expression of NES-Clb3Δ130 is not the only factor that facilitates the degradation of degron module conjugated proteins and it has been thought that regular Clb3 expression of the strain might lead to such leakage. Besides, it has also been shown that in the state of NES-Clb3Δ130 expression the protein level of CIT2 drops independently from the identity of tagging module it has been conjugated to which means that the system is not orthogonal.

In conclusion, the study on Clb3-CDC28 specific degron module established that the degradation of such degron module conjugated protein is controllable, while the handicaps of the system could be improved in order to reach desired controllable protein degradation system.

REFERENCES

Adams, P. D., Li, X., Sellers, W. R., Baker, K. B., Leng, X., Harper, J. W., Taya, Y., & Kaelin, W. G. (1999). *Retinoblastoma Protein Contains a C-terminal Motif That Targets It for Phosphorylation by Cyclin-cdk Complexes*. *19*(2), 1068–1080.

Alto, P. (1995). *Cyclin dependent kinase regulation*.

Amon, A., Tyers, M., Futcher, B., & Nasmyth, K. (1993). Mechanisms that help the yeast cell cycle clock tick: G2 cyclins transcriptionally activate G2 cyclins and repress G1 cyclins. *Cell*, *74*(6), 993–1007. https://doi.org/10.1016/0092-8674(93)90722-3

Barberis, M. (2012). Sic1 as a timer of Clb cyclin waves in the yeast cell cycle - Design principle of not just an inhibitor. *FEBS Journal*, *279*(18), 3386–3410. https://doi.org/10.1111/j.1742-4658.2012.08542.x

Basco, R. D., Segal, M. D., & Reed, S. I. (1995). Negative regulation of G1 and G2 by S-phase cyclins of Saccharomyces cerevisiae. *Molecular and Cellular Biology*, *15*(9), 5030–5042. https://doi.org/10.1128/mcb.15.9.5030

Berset, C., Griac, P., Tempel, R., La Rue, J., Wittenberg, C., & Lanker, S. (2002). Transferable Domain in the G1 Cyclin Cln2 Sufficient To Switch Degradation of Sic1 from the E3 Ubiquitin Ligase SCFCdc4 to SCFGrr1. *Molecular and Cellular Biology*, *22*(13), 4463–4476. https://doi.org/10.1128/mcb.22.13.4463-4476.2002

Bhaduri, S., & Pryciak, P. M. (2011). Article Cyclin-Specific Docking Motifs Promote Phosphorylation of Yeast Signaling Proteins by G1 / S Cdk Complexes. *Current Biology*, *21*(19), 1615–1623. https://doi.org/10.1016/j.cub.2011.08.033

Blake, C. M., & Cross, F. R. (1993). *The Yeast Cln3 Protein Is Unstable Activator of Cdc28*. *13*(6), 3266–3271.

Blondel, M. (2000). Nuclear-specific degradation of Far1 is controlled by the localization of the F-box protein Cdc4. *The EMBO Journal*, *19*(22), 6085–6097. https://doi.org/10.1093/emboj/19.22.6085

Bloom, J., & Cross, F. R. (2007). *Multiple levels of cyclin specificity in cell-cycle control*. *8*(February), 149–160. https://doi.org/10.1038/nrm2105

Chulman, B. R. A. S., & Indstrom, D. E. L. L. (1998). *Substrate recruitment to cyclin-dependent kinase 2 by a multipurpose docking site on cyclin A*. *95*(September), 10453–10458.

Cohen, P. (2002). *The origins of protein phosphorylation*. *4*(May).

Cross, F. F. (1991). *A Potential Positive Feedback Loop Controlling CL / VI and CL / V2 Gene Expression at the Start of the Yeast Cell Cycle*. *65*, 875–883.

Cross, F. R. (1988). *DAFJ , a Mutant Gene Affecting Size Control , Pheromone Arrest , and Cell Cycle Kinetics of Saccharomyces cerevisiae i L*. *8*(11), 4675–4684.

Cross, F. R. (2003). *Two Redundant Oscillatory Mechanisms in the Yeast Cell Cycle*. *4*, 741–752.

Cross, F. R., Yuste-Rojas, M., Gray, S., & Jacobson, M. D. (1999). Specialization and targeting of B-type cyclins. *Molecular Cell*, *4*(1), 11–19. https://doi.org/10.1016/S1097-2765(00)80183-5

Deshaies, R. J. (1999). */ring h2-b*.

Dingwall C, & Laskey RA. (1991). Nuclear target sequences a consensus? *Tibs*, *December*, 478–481.

Dirick, L., Bohm, T., & Nasmyth, K. (1995). *Roles and regulation of Cln-Cdc28 kinases at the start of the cell cycle of Saccharomyces cerevisiae*. *14*(19), 4803–4813.

Drury, L. S., Perkins, G., & Diffley, J. F. X. (1997). The Cdc4/34/53 pathway targets Cdc6p for proteolysis in budding yeast. *EMBO Journal*, *16*(19), 5966–5976. https://doi.org/10.1093/emboj/16.19.5966

Edgington, N. P., & Futcher, B. (2001). Relationship between the function and the location of G1 cyclins in S. cerevisiae. *Journal of Cell Science*, *114*(24), 4599–4611.

Epstein, C. B., & Cross, F. R. (1992). *CLB5 : a novel B cyclinfrom budding yeast with a role in S phase*. 1695–1706.

Feldman, R. M. R., Correll, C. C., Kaplan, K. B., & Deshaies, R. J. (1997). A complex of Cdc4p, Skp1p, and Cdc53p/cullin catalyzes ubiquitination of the phosphorylated CDK inhibitor Sic1p. *Cell*, *91*(2), 221–230. https://doi.org/10.1016/S0092-8674(00)80404-3

Fitch, I., Dahmann, C., Surana, U., Amon, A., Nasmyth, K., Goetsch, L., Byers, B., & Futcher, B. (1992). *Characterization of Four B-Type Cyclin Genes of the Budding Yeast Saccharomyces cerevisiae*. *3*(July), 805–818.

Galderisi, U., Jori, F. P., & Giordano, A. (2003). *Cell cycle regulation and neural differentiation*. 5208–5219. https://doi.org/10.1038/sj.onc.1206558

Ghiara, J. B., Richardson, H. E., Sugimoto, K., Henze, M., Lew, D. J., Wittenberg, C., & Reed, S. I. (1991). *A Cyclin B Homolog in S . cerevisiae : Chronic Activation of the Cdc28 Protein Kinase by Cyclin Prevents Exit from Mitosis*. 163–174.

Grandin, N., & Reed, S. I. (1993). Differential function and expression of Saccharomyces cerevisiae B-type cyclins in mitosis and meiosis. *Molecular and Cellular Biology*, *13*(4), 2113–2125. https://doi.org/10.1128/mcb.13.4.2113

Haas, A. L., Warms, J. V. B., Hershkog, A., & Rose, I. A. (1982). *Ubiquitin-activating Enzyme*. *257*(5).

Henchoz, S., Chi, Y., Catarin, B., Herskowitz, I., Deshaies, R. J., & Peter, M. (1997). *Phosphorylation- and ubiquitin-dependent degradation of the cyclin-dependent kinase inhibitor Far1p in budding yeast*. 3046–3060.

Hsiung, Y. G., Chang, H.-C., Pellequer, J.-L., La Valle, R., Lanker, S., & Wittenberg, C. (2001). F-Box Protein Grr1 Interacts with Phosphorylated Targets via the Cationic Surface of Its Leucine-Rich Repeat. *Molecular and Cellular Biology*, *21*(7), 2506–2520. https://doi.org/10.1128/mcb.21.7.2506-2520.2001

Hurley, J. H., Lee, S., & Prag, G. (2006). Ubiquitin-binding domains. *Biochemical Journal*, *399*(3), 361–372. https://doi.org/10.1042/BJ20061138

Janke, C., Magiera, M. M., Rathfelder, N., Taxis, C., & Reber, S. (2004). *A versatile toolbox for PCR-based tagging of yeast genes : new fluorescent proteins , more*. 947–962. https://doi.org/10.1002/yea.1142

Jaquenoud, M., Gulli, M., Peter, K., & Peter, M. (1998). *The Cdc42p effector Gic2p is targeted for ubiquitin-dependent degradation by the SCF Grr1 complex*. *17*(18), 5360–5373.

Jolla, L. (2021). *Cyclin-B h0mologs ! n Saccharomyc . es cerevisiae function in S phase and m G2*. 2021–2034.

Kishi, T., & Yamao, F. (1998). An essential function of Grr1 for the degradation of Cln2 is to act as a binding core that links Cln2 to Skp1. *Journal of Cell Science*, *111*(24), 3655–3661.

Kõivomägi, M., Örd, M., Iofik, A., Valk, E., Venta, R., & Faustova, I. (2014). *Europe PMC Funders Group Multisite phosphorylation networks as signal processors for*. *20*(12), 1–24. https://doi.org/10.1038/nsmb.2706.Multisite

Kõivomägi, M., Valk, E., Venta, R., Iofik, A., Lepiku, M., Morgan, D. O., & Loog, M. (2011). Dynamics of Cdk1 Substrate Specificity during the Cell Cycle. *Molecular Cell*, *42*(5), 610–623. https://doi.org/10.1016/j.molcel.2011.05.016

Kuhne, C., & Linder, P. (1993). *pair of B-type cyclins from Saccharomyces cerevisiae that function early in the cell cycle new*. *12*(9), 3437–3447.

Landry, B. D., Doyle, J. P., Toczyski, D. P., & Benanti, J. A. (2012). F-box protein specificity for G1 cyclins is dictated by subcellular localization. *PLoS Genetics*, *8*(7). https://doi.org/10.1371/journal.pgen.1002851

Lanker, S., Valdivieso, M. H., & Wittenberg, C. (1996). Rapid degradation of the G1 cyclin Cln2 induced by CDK-Dependent phosphorylation. *Science*, *271*(5255), 1597–1601. https://doi.org/10.1126/science.271.5255.1597

Levine, K., Huang, K., & Cross, F. R. (1996). *Saccharomyces cerevisiae G 1 Cyclins Differ in Their Intrinsic Functional Specificities*. *16*(12), 6794–6803.

Lew, D. J., Dulic, V., & Reed, S. I. (1991). *Isolation of Three Novel Human Cyclins by Rescue of Gl Cyclin (Cln) Function in Yeast*. *66*, 1197–1206.

Lim, S., & Kaldis, P. (2013). *Cdks , cyclins and CKIs : roles beyond cell cycle regulation*. *3093*, 3079–3093. https://doi.org/10.1242/dev.091744

Loog, M. (2011). *Cascades of multisite phosphorylation control Sic1 destruction at the onset of S phase*. 0–4. https://doi.org/10.1038/nature10560

Loog, M., & Morgan, D. O. (2005). Cyclin specificity in the phosphorylation of cyclin-dependent kinase substrates. *Nature*, *434*(7029), 104–108. https://doi.org/10.1038/nature03329

Magill, J. C., Byl, M. F., Goldwaser, B., Instructor, M. P., Yates, B., Morency, J. R., Kaban, L. B., Guralnick, W. C., & Associate, M. J. T. (2010). *Cks Confers Specificity to Phosphorylation-Dependent Cdk Signaling Pathways Denise*. *3*(1), 1–19. https://doi.org/10.1115/1.3071969.Automating

Malumbres, M., Harlow, E., Hunt, T., Hunter, T., Lahti, J. M., Manning, G., Morgan, D. O., Tsai, L. H., & Wolgemuth, D. J. (2009). Cyclin-dependent kinases: A family portrait. *Nature Cell Biology*, *11*(11), 1275–1276. https://doi.org/10.1038/ncb1109-1275

Mann, C., & Commission, A. E. (2015). *G1 cyclin turnover and nutrient uptake are controlled by a common pathway in yeast G1 cyclin turnover and nutrient uptake are controlled by a common pathway in yeast . December*. https://doi.org/10.1101/gad.9.4.399

Manuscript, A. (2015). *NIH Public Access*. *14*(4), 233–247. https://doi.org/10.1038/nrc3700.Roles

Mcgrath, J. P., Jentsch, S., & Varshavsky, A. (1991). *Uba 1: 10*(1), 227–236. https://doi.org/10.1002/j.1460-2075.1991.tb07940.x

Mendenhall, M. D., & Hodge, A. E. (1998). Regulation of Cdc28 Cyclin-Dependent Protein Kinase Activity during the Cell Cycle of the Yeast Saccharomyces cerevisiae. *Microbiology and Molecular Biology Reviews*, *62*(4), 1191–1243. https://doi.org/10.1128/mmbr.62.4.1191-1243.1998

Miller, M. E., & Cross, F. R. (2000). Distinct Subcellular Localization Patterns Contribute to Functional Specificity of the Cln2 and Cln3 Cyclins of Saccharomyces cerevisiae. *Molecular and Cellular Biology*, *20*(2), 542–555. https://doi.org/10.1128/mcb.20.2.542-555.2000

Miller, M. E., & Cross, F. R. (2001). Mechanisms Controlling Subcellular Localization of the G1 Cyclins Cln2p and Cln3p in Budding Yeast. *Molecular and Cellular Biology*, *21*(18), 6292–6311. https://doi.org/10.1128/mcb.21.18.6292-6311.2001

Morgan, D. O. (2007). *Primers in Biology The Cell Cycle Primers in Biology : Protein Structure and Function Forthcoming titles :*

Morgan, D. O., & Roberts, J. M. (2002). *Cell cycle Oscillation sensation*. *418*(August), 1–2.

Ohta, T., Michel, J. J., Schottelius, A. J., Xiong, Y., Hill, C., & Carolina, N. (1999). *ROC1 , a Homolog of APC11 , Represents a Family of Cullin Partners with an Associated Ubiquitin Ligase Activity University of North Carolina at Chapel Hill*. *3*, 535–541.

Örd, M., & Loog, M. (2019). How the cell cycle clock ticks. *Molecular Biology of the Cell*, *30*(2), 169–172. https://doi.org/10.1091/mbc.E18-05-0272

Örd, M., Möll, K., Agerova, A., Kivi, R., Faustova, I., Venta, R., & Valk, E. (2020). *Europe PMC Funders Group Multisite phosphorylation code of CDK*. *26*(7), 649–658. https://doi.org/10.1038/s41594-019-0256-4.Multisite

Orlicky, S., Tang, X., Willems, A., Tyers, M., & Sicheri, F. (2003). Structural basis for phosphodependent substrate selection and orientation by the SCFCdc4 ubiquitin ligase. *Cell*, *112*(2), 243–256. https://doi.org/10.1016/S0092-8674(03)00034-5

Ottoz, D. S. M., Rudolf, F., & Stelling, J. (2014). *Inducible , tightly regulated and growth condition-independent transcription factor in Saccharomyces cerevisiae*. *42*(17). https://doi.org/10.1093/nar/gku616

Patton, E. E., Willems, A. R., Sa, D., Kuras, L., Thomas, D., Craig, K. L., & Tyers, M. (1998). *Cdc53 is a scaffold protein for multiple complexes that regulate cell division and methionine biosynthesis in yeast*. 692–705.

Pickart, C. M. (2001). *Echanisms nderlying biquitination*.

Positive feedback in the activation of G1 cyclins in yeast.pdf. (n.d.).

Rechsteiner, M., & Rogers, S. W. (1996). PEST sequences and regulation by proteolysis. *Trends in Biochemical Sciences*, *21*(7), 267–271. https://doi.org/10.1016/S0968-0004(96)10031-1

Rédei, G. P. (2008). Cks1. *Encyclopedia of Genetics, Genomics, Proteomics and Informatics*, *4*(8), 369–369. https://doi.org/10.1007/978-1-4020-6754-9_3107

Reed, S. I. (2003). Ratchets and clocks: The cell cycle, ubiquitylation and protein turnover. *Nature Reviews*

Molecular Cell Biology, *4*(11), 855–864. https://doi.org/10.1038/nrm1246

Rev, A., Dev, C., Downloaded, B., & Morgan, D. O. (1997). *CYCLIN-DEPENDENT KINASES : Engines , Clocks , and Microprocessors*.

Salama, S. R., Hendricks, K. B., & Thorner, J. (1994). G1 cyclin degradation: the PEST motif of yeast Cln2 is necessary, but not sufficient, for rapid protein turnover. *Molecular and Cellular Biology*, *14*(12), 7953–7966. https://doi.org/10.1128/mcb.14.12.7953

Schwob, E. (1993). *CLB5 and CLB6 , a new pair of B cyclins involved in D N A replication in Saccharom yces cereHsiae*. 1160–1175.

Schwob, E., Thomas, B., Mendenhall, M. D., & Nasmyth, K. (1994). *The B-Type Cyclin Kinase Inhibitor p4 @ ' Controls the G l to S Transition in S . cerevisiae*. *79*, 233–244.

Seol, J. H., Feldman, R. M. R., Zachariae, W., Shevchenko, A., Correll, C. C., Lyapina, S., Chi, Y., Galova, M., Claypool, J., Sandmeyer, S., Nasmyth, K., Shevchenko, A., & Deshaies, R. J. (1999). Cdc53/cullin and the essential Hrt1 RING-H2 subunit of SCF define a ubiquitin ligase module that activates the E2 enzyme Cdc34. *Genes and Development*, *13*(12), 1614–1626. https://doi.org/10.1101/gad.13.12.1614

Skotheim, J. M. (2019). *Docking Interactions : Cell-Cycle Regulation and Beyond*. *24*(14), 10–13. https://doi.org/10.1016/j.cub.2014.05.060.Docking

Skotheim, J. M., Talia, S. Di, Siggia, E. D., & Cross, F. R. (2009). *entry*. *454*(7202), 291–296. https://doi.org/10.1038/nature07118.Positive

Skowyra, D., Craig, K. L., Tyers, M., Elledge, S. J., & Harper, J. W. (1997). F-box proteins are receptors that recruit phosphorylated substrates to the SCF ubiquitin-ligase complex. *Cell*, *91*(2), 209–219. https://doi.org/10.1016/S0092-8674(00)80403-1

Songyang, Z., Blechner, S., Hoagland, N., Hoekstra, M. F., Piwnica-Worms, H., & Cantley, L. C. (1994). Use of an oriented peptide library to determine the optimal substrates of protein kinases. *Current Biology*, *4*(11), 973–982. https://doi.org/10.1016/S0960-9822(00)00221-9

Spellman, P. T., Sherlock, G., Zhang, M. Q., Vishwanath, R., Anders, K., Eisen, M. B., Brown, P. O., & Futcher, B. (1998). *Comprehensive Identification of Cell Cycle – regulated Genes of the Yeast Saccharomyces cerevisiae by Microarray Hybridization □*. *9*(December), 3273–3297.

Stueland, C. S., Lew, D. J., Cismowski, M. J., & Reed, S. I. (1993). *Full Activation of p34CDC28 Histone Hi Kinase Activity Is Unable To Promote Entry into Mitosis in Checkpoint- Arrested Cells of the Yeast Saccharomyces cerevisiae*. *13*(6), 3744–3755.

Surana, U., Robitsch, H., Price, C., Schuster, T., Fitch, I., Futcher, A. B., & Nasmyth, K. (1991). The role of CDC28 and cyclins during mitosis in the budding yeast S. cerevisiae. *Cell*, *65*(1), 145–161. https://doi.org/10.1016/0092-8674(91)90416-V

Swaffer, M. P., Jones, A. W., Flynn, H. R., Snijders, A. P., & Nurse, P. (2016). CDK Substrate Phosphorylation and Ordering the Cell Cycle. *Cell*, *167*(7), 1750-1761.e16. https://doi.org/10.1016/j.cell.2016.11.034

Tang, Y., & Reed, S. I. (1993). The Cdk-associated protein Cks1 functions both in G1 and G2 in Saccharomyces cerevisiae. *Genes and Development*, *7*(5), 822–832. https://doi.org/10.1101/gad.7.5.822

Tyers, M., Tokiwa, G., & Futcher, B. (1993). *Comparison of the Saccharomyces cerevisiae G1 cyclins : Cln3 may be an upstream activator of Clnl , Cln2 and other cyclins*. *12*(5), 1955–1968.

Ubersax, J. A., & Jr, J. E. F. (2007). *Mechanisms of specificity in protein phosphorylation*. *8*(July), 530–542. https://doi.org/10.1038/nrm2203

Valk, E., Venta, R., Iofik, A., Lepiku, M., M, E. R., Rubin, S. M., Morgan, D. O., Loog, M., Cruz, S., & Francisco, S. (2012). *HHS Public Access*. *480*(7375), 128–131. https://doi.org/10.1038/nature10560.Cascades

Verma, R., Feldman, R. M. R., & Deshaies, R. J. (1997). *SICI Is Ubiquitinated In Vitro by a Pathway that*. *8*(August), 1427–1437.

Vlastaridis, P., Kyriakidou, P., Chaliotis, A., Peer, Y. Van De, Oliver, S. G., & Amoutzias, G. D. (2017). *Estimating the total number of phosphoproteins and phosphorylation sites in eukaryotic proteomes*. *December 2016*, 1–11. https://doi.org/10.1093/gigascience/giw015

Vodermaier, H. C. (2004). APC/C and SCF: Controlling each other and the cell cycle. *Current Biology*, *14*(18), 787–796. https://doi.org/10.1016/j.cub.2004.09.020

Wei, L., & Yihong, Y. (2009). *NIH Public Access*. *65*(15), 2397–2406. https://doi.org/10.1007/s00018-008-8090-6.Polyubiquitin

Willems, A. R., Schwab, M., & Tyers, M. (2004). A hitchhiker's guide to the cullin ubiquitin ligases: SCF and its kin. *Biochimica et Biophysica Acta - Molecular Cell Research*, *1695*(1–3), 133–170. https://doi.org/10.1016/j.bbamcr.2004.09.027

Wilmes, G. M., Archambault, V., Austin, R. J., Jacobson, M. D., Bell, S. P., & Cross, F. R. (2004). *Interaction of the S-phase cyclin Clb5 with an ' RXL ' docking sequence in the initiator protein Orc6 provides an origin-localized replication control switch*. 981–991. https://doi.org/10.1101/gad.1202304.of

Xie, J., Jin, Y., & Wang, G. (2019). The role of SCF ubiquitin-ligase complex at the beginning of life. *Reproductive Biology and Endocrinology*, *17*(1), 1–9. https://doi.org/10.1186/s12958-019-0547-y

Xu, D., Farmer, A., Collett, G., Grishin, N. V, & Min, Y. (2012). *Sequence and structural analyses of nuclear export signals in the NESdb database*. *23*. https://doi.org/10.1091/mbc.E12-01-0046

Yaglom, J., Linskens, M. H., Sadis, S., Rubin, D. M., Futcher, B., & Finley, D. (1995). p34Cdc28-mediated control of Cln3 cyclin degradation. *Molecular and Cellular Biology*, *15*(2), 731–741. https://doi.org/10.1128/mcb.15.2.731

Zacksenhaus, E., & Sheinin, R. (1990). *Molecular cloning , primary structure and expression of the human X linked AlS9 gene cDNA which complements the ts A1S9 mouse L cell defect in DNA replication*. *9*(9), 2923–2929. https://doi.org/10.1002/j.1460-2075.1990.tb07483.x

NON-EXCLUSIVE LICENSE TO REPRODUCE THESIS AND MAKE THESIS PUBLIC

I, Turan Badalli,

1. herewith grant the University of Tartu a free permit (non-exclusive licence) to:

1.1. reproduce, for the purpose of preservation, including for adding to the DSpace digital archives until the expiry of the term of copyright, and

1.2. make available to the public via the web environment of the University of Tartu, including via the DSpace digital archives, under the Creative Commons licence CC BY NC ND 3.0, which allows, by giving appropriate credit to the author, to reproduce, distribute the work and communicate it to the public, and prohibits the creation of derivative works and any commercial use of the work from 20/05/2023 until the expiry of the term of copyright,

Inducible protein degradation in Saccharomyces cerevisiae,

supervised by Rait Kivi PhD and Kaidi Möll MSc,

2. I am aware of the fact that the author retains the rights specified in p. 1.

3. I certify that granting the non-exclusive licence does not infringe other persons' intellectual property rights or rights arising from the personal data protection legislation.

Turan Badalli

20/05/2020

SUPPLEMENTARY MATERIAL

Synthetic DNA	Sequence
synth DNA Sic1 TTT AAAA PNF 3HA	TGCATGGATCCATGAACGAATTAGCTTTAAAGCTGGCAGGCTTGGACATCAATAAAATGAC GCCCAGCACGCCACCAAGGTCTCGTGGAACCAGATACTTAGCGCAGCCATCTGGTAACAC GTCCAGTTCTGCTTTAATGCAGGGACAAAAGACCCCACAGAAGCCGTCTCAGAACTTAGTT CCTGTCTCCATTCCTgcgCCCGCTTCCTCATCTCAAAGCCACgcgCCAATGAGAAACATGAGC TCACTCTCTGATAACAGCGTTTTCAGCCGGAATATGGAACAATCAgcgCCAATCgcgCCAAGT ATGTACCAATTTGGTCAGCAGCAGTCAAACAGTATATGTCCCCCAAAGGGtCCtAAtTTCTA CGCCAAGGAGTCCCACGACAACGGGACCGTCAGAGAAGAGCAAGAACCTTTACCCCCAAA GGGCCCCAACTTCTACGCCAAGCAGCAGAACGTGGATATAGATGCTGCCGAGGAAGAAG AGGAAGGTGAGGCTGCGGCTGCCGCCTCCAGGCCAACATCAGCGAGACAACTGCATTTAT CACTTGAAAGAGACGAGTTCGACCAAACGCACCGTAAGAAGATTATTAAGGATGTGCCGG GAGCCCCATCTGATAAGGTCATTACCTTTGAACTTGCCAAAAACTGGAACAATAATGCCCC GAAAAATGACGCGCGTTCTCAAGAAAGTGAAGACGAAGAAGACATAATAATTAACCCTGT TAGGGTTGGATACCCGTATGACGTTCCGGATTACGCTTATCCATATGATGTCCCAGACTAT GCGTATCCGTACGATGTACCCGATTATGCGTAAGCGGCCGCATGCAT
synth DNA Sic1 TTT STST PNF 3HA	AAGCATGGATCCATGAACGAATTAGCTTTAAAGCTGGCAGGCTTGGACATCAATAAAATG ACGCCCAGCACGCCACCAAGGTCTCGTGGAACCAGATACTTAGCGCAGCCATCTGGTAAC ACGTCCAGTTCTGCTTTAATGCAGGGACAAAAGACCCCACAGAAGCCGTCTCAGAACTTAG TTCCTGTCTCCATTCCTTCGCCCGCTTCCTCATCTCAAAGCCACACTCCAATGAGAAACATGA GCTCACTCTCTGATAACAGCGTTTTCAGCCGGAATATGGAACAATCATCACCAATCACTCCA AGTATGTACCAATTTGGTCAGCAGCAGTCAAACAGTATATGTCCCCCAAAGGGtCCtAAtTT CTACGCCAAGGAGTCCCACGACAACGGGACCGTCAGAGAAGAGCAAGAACCTTTACCCCC AAAGGGCCCCAACTTCTACGCCAAGCAGCAGAACGTGGATATAGATGCTGCCGAGGAAGA AGAGGAAGGTGAGGCTGCGGCTGCCGCCTCCAGGCCAACATCAGCGAGACAACTGCATTT ATCACTTGAAAGAGACGAGTTCGACCAAACGCACCGTAAGAAGATTATTAAGGATGTGCC GGGAGCCCCATCTGATAAGGTCATTACCTTTGAACTTGCCAAAAACTGGAACAATAATGCC CCGAAAAATGACGCGCGTTCTCAAGAAAGTGAAGACGAAGAAGACATAATAATTAACCCT GTTAGGGTTGGATACCCGTATGACGTTCCGGATTACGCTTATCCATATGATGTCCCAGACT ATGCGTATCCGTACGATGTACCCGATTATGCGTAAGCGGCCGCATGCAT
linker_3HA	gctgcaggtcgacggtggtggaggctctggaggtggtggaggttctggcggtggaggtggttcaTACC CGTATGACGTTCCGGATTACGCTTATCCATATGATGTCCCAGACTATGC GTATCCGTACGATGTACCCGATTATGCGtagggcgcgccagatct